CHAPTER 5

ABC REFERENCE FRAME CONTROLLER

5.1 Introduction

There are situations in which it is desirable to impress an unbalanced three-phase voltage set to an unbalanced three-phase load in order to ensure a balanced three-phase load current or to use unbalanced three-phase voltage set for voltage or current compensation in active filters in distribution lines. Some fault situations in electric machines and generators manifest as unequal phase impedances or unbalanced induced voltages. In general, four-leg inverters may be used in such applications since the phase currents are not constrained when the star point of the three-phase load is connected to a fourth neutral wire. However when the impressed unbalanced three-phase voltage set is constrained such that the load currents add to zero in star-connected loads, a three-leg inverter can be used. Under such conditions, the expressions for the three modulation signals M_{ip} required to turn on or turn off the switches must be determined given the phase voltages v_{an} , $v_{bn,}$ v_{cn} which are not balanced in general.

This chapter proposes an algorithm to control the currents of an unbalanced three-phase load using pulse-width modulation (PWM) based converters. The approach develops a controller compensation technique and modulation signals required to turn on/switch off the switches to obtain the balanced phase currents irrespective of a

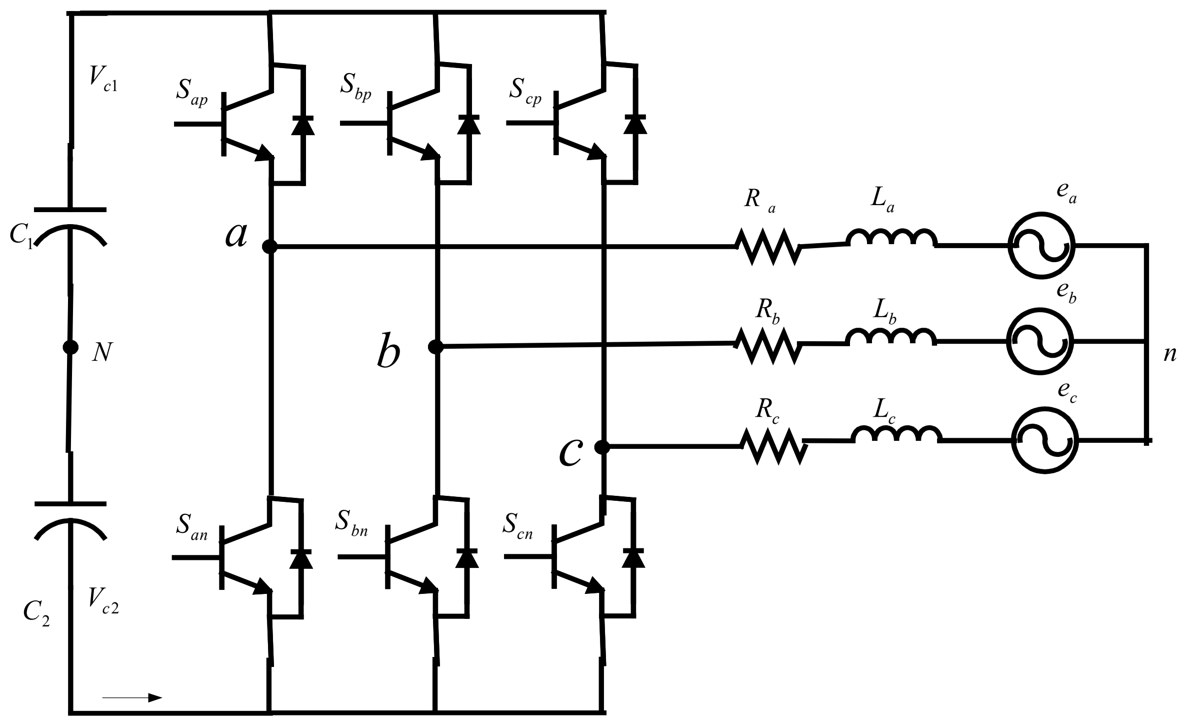

Figure 5.1: Three Phase Unbalanced System.

balanced or unbalanced load. The modeling of the unbalanced load system and detailed controller design methodology are set forth.

5.2 Model of the Three-Phase Load

In Figure 5.1, the circuit represents a typical three-phase unbalanced system. v_{aN}, v_{bN}, v_{cN} are the phase output voltages of a three phase voltage source inverter and e_a, e_b, and e_c are the induced voltages in the load and the general impedances of the load are shown. This load may be balanced or unbalanced.

From the Figure 5.1 it is clear that

$$v_{aN} = v_{an} + v_{nN} \tag{5.1}$$

$$v_{bN} = v_{bn} + v_{nN} \tag{5.2}$$

$$v_{cN} = v_{cn} + v_{nN} \tag{5.3}$$

where

$$v_{an} = i_a R_a + L_a pi_a + e_a \tag{5.4}$$

$$v_{bn} = i_b R_b + L_b pi_b + e_b \tag{5.5}$$

$$v_{cn} = i_c R_c + L_c pi_c + e_c\,. \tag{5.6}$$

Consider,

$$v_{aN} - v_{aN} = i_a R_a + L_a pi_a + e_a - (i_b R_b + L_b pi_b + e_b)\,. \tag{5.7}$$

Similarly,

$$v_{bN} - v_{cN} = i_b R_b + L_b pi_b + e_b - (i_c R_c + L_c pi_c + e_c)\,. \tag{5.8}$$

From the current balance equation, $i_c = -(i_a + i_b)$. (5.9)

Substituting i_c in 5.8 and simplifying

$$v_{bN} - v_{cN} = i_b (R_b + R_c) + (L_b + L_c) pi_b + e_b + i_a R_c + L_c pi_a - e_c\,. \tag{5.10}$$

By solving the above two equations for pI_a and pI_b

$$pi_a = \frac{(-R_a i_a L_b - R_a i_a L_c - R_c i_b L_b - (v_{aN} - e_c) L_b - R_c i_a L_b + (v_{aN} - e_a) L_b + (v_{aN} - e_a) L_c - (v_{bN} - e_b) L_c + R_b i_b L_c}{L_a L_b + L_a L_c + L_c L_b}$$

$$= \sigma_b \qquad \text{(5.11-a)}$$

$$pi_b = \frac{-(R_b i_b L_b + R_c i_b L_a - (v_{bN} - e_b) L_a + (v_{bN} - e_b) L_a + (v_{aN} - e_a) L_c - (v_{bN} - e_b) L_c + R_c i_a L_a - R_a i_a L_c + R_b i_b L_c}{L_a L_b + L_a L_c + L_c L_b}$$

$$= \sigma_b. \qquad \text{(5.11-b)}$$

In case of balance load conditions i.e., $R_a = R_b = R_c = R$, $L_a = L_b = L_c = L$, and

$e_a = e_b = e_c = E$

$$pi_a = \frac{-3Ri_a + 2v_{aN} - v_{bN} - v_{cN}}{3L} = \sigma_a \qquad \text{(5.12-a)}$$

$$pi_b = \frac{-3Ri_b + 2v_{bN} - v_{aN} - v_{cN}}{3L} = \sigma_b. \tag{5.12-b}$$

5.3 Control Scheme

In this particular scheme the current is controlled to obtain three phase balanced load current under unbalanced load conditions. The following block diagram represents the schematic of the control scheme.

The scheme works as follows: The voltage source inverter is connected to an arbitrary load. The main criterion of this scheme is to balance the three phase currents irrespective of what the load is. The control is based on using natural variables of the system without any transformation. In the control scheme the phase currents i_a, i_b, and i_c used as feedback signals are compared with the reference currents which are defined. The error current is then passed through the controller whose structure is described in the following section. The outputs of the controllers are taken as the derivatives of the phase

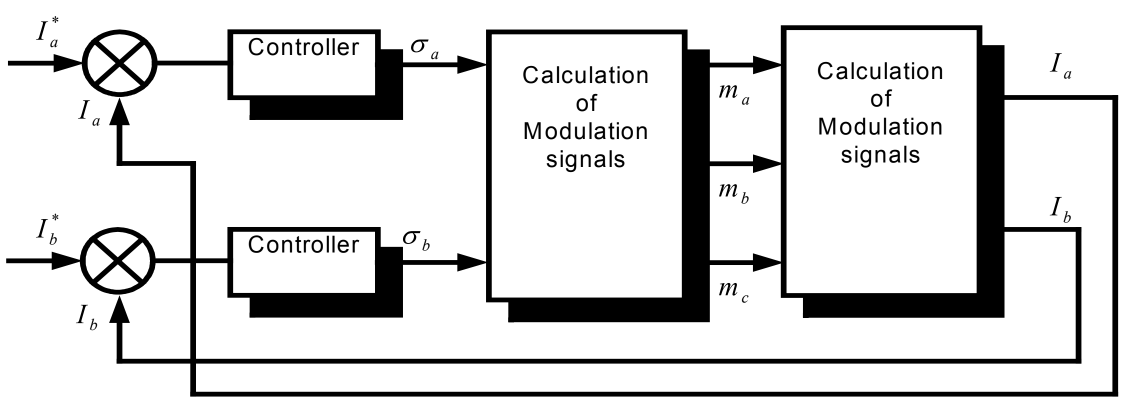

Figure 5.2: Block diagram of the control scheme

currents. Only two controllers are used and the third reference current is obtained from the balance equation of the current, since

$$i_a + i_b + i_c = 0$$
$$\Rightarrow i_c = -(i_a + i_b)$$
$$\text{Also, } pi_c = -(pi_b + pi_c). \tag{5.13}$$

Using the outputs of the controllers and using Equations (5.4-5.6), the reference phase voltages, which are used to generate the modulating signals to be described in Section 5.5.

5.3.1 Structure of the Controller

The block diagram of the controller is outlined in Figure 5.3. The currents of the inverter are being controlled and hence the inverter currents are used as the feedback signals. The currents i_a, i_b, are taken from the inverter and are compared with the reference current signals i_a^*, i_b^*.

The errors of the currents are converted to positive and negative synchronous reference frames; i.e., θ_x and $-\theta_x$. Hence the output of the transformation block is

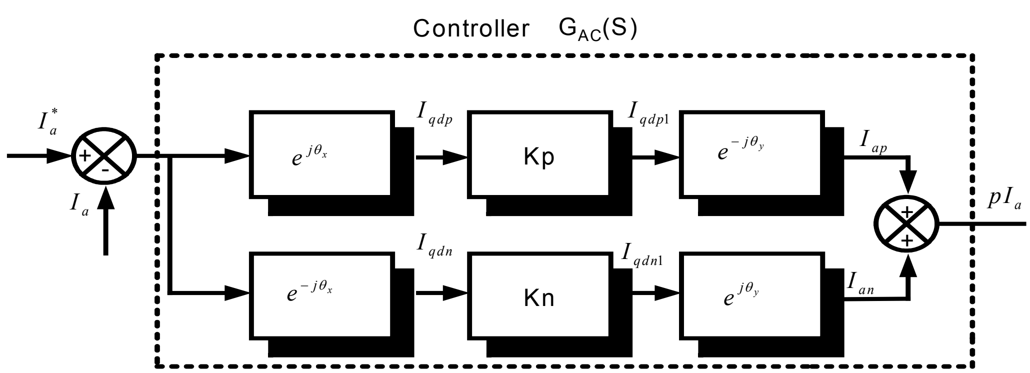

Figure 5.3: Structure of the controller

$$i_{qdp} = (i_a^* - i_a)e^{i\theta_x} \tag{5.14}$$

$$i_{qdn} = (i_a^* - i_a)e^{-i\theta_x} \tag{5.15}$$

where $\theta_x = \omega_e t + \theta_{x0}$; θ_{x0} - Initial reference angle.

These signals are considered to be constant after the transformations. These signals are passed through two controllers whose transfer functions are given by K_p (p) and K_n (p). Hence the output of the regulators is

$$i_{qdp1} = (i_a^* - i_a)e^{i\theta_x} K_p(p) \tag{5.16}$$

$$i_{qdn} = (i_a^* - i_a)e^{-i\theta_x} K_n(p)\,. \tag{5.17}$$

Now these signals are again transformed back to the abc reference frame with some delay angle ϕ_1 i.e., $\theta_y = \omega_e t + \theta_{x0} - \phi_1, \theta_y = -\omega_e t + \theta_{x0} - \phi_1$. Hence the resulting signals from these transformation blocks are

$$i_{ap} = (i_a^* - i_a)e^{i(\theta_x - \theta_y)} K_p(p - j\omega) \tag{5.18}$$

$$i_{an} = (i_a^* - i_a)e^{-i(\theta_x - \theta_y)} K_n(p + j\omega)\,. \tag{5.19}$$

Let $\theta_x - \theta_y = \phi_1$, then

$$i_{ap} = (i_a^* - i_a)e^{i\phi_1} K_p(p - j\omega) \tag{5.20}$$

$$i_{an} = (i_a^* - i_a)e^{-i\phi_1} K_n(p + j\omega)\,. \tag{5.21}$$

The sum of the two signals i_{ap}, i_{an} is taken to get the output of the controller, which is equal to pi_a.

$$pi_a = (i_a^* - i_a)e^{i\phi_1} K_p(p - j\omega) + (i_a^* - i_a)e^{-i\phi_1} K_n(p + j\omega)$$

$$\Rightarrow (i_a^* - i_a)[e^{i\phi_1} K_p(p - j\omega) + e^{-i\phi_1} K_n(p + j\omega)]$$

By simplifying the above equation, the transfer function of the system is obtained as

$$\frac{i_a}{i_a^*} = \frac{e^{i\phi_1} K_p(p - j\omega) + e^{-i\phi_1} K_n(p + j\omega)}{p + e^{i\phi_1} K_p(p - j\omega) + e^{-i\phi_1} K_n(p + j\omega)}. \tag{5.22}$$

In this particular case, assume the controller to be a PI controller whose transfer function is given as

$$\begin{aligned} K_p(p) &= k_p + \frac{k_{ip}}{p} \\ K_n(p) &= k_n + \frac{k_{in}}{p}. \end{aligned} \tag{5.23}$$

Hence, by substituting the above transfer functions in Eq. (5.22) and simplifying

$$\frac{i_a}{i_a^*} = \frac{e^{i\phi_1}(p + j\omega)[k_p(p - j\omega) + k_{ip}] + e^{-i\phi_1}(p - j\omega)[k_n(p + j\omega) + k_{in}]}{p(p^2 + \omega^2) + e^{i\phi_1}(p + j\omega)[k_p(p - j\omega) + k_{ip}] + e^{-i\phi_1}(p - j\omega)[k_n(p + j\omega) + k_{in}]}.$$

For simplicity, if $k_{ip} = k_{in} = k_i ; k_n = k_p = k_p$, then

$$\frac{i_a}{i_a^*} = \frac{p^2 2k_p \cos\phi_1 + p2k_i \cos\phi_1 + 2\cos\phi_1\omega^2 k_p - 2k_i\omega\sin\phi_1}{p^3 + p^2 2k_p \cos\phi_1 + p[2k_i \cos\phi_1 + \omega^2] + 2\cos\phi_1\omega^2 k_p - 2k_i\omega\sin\phi_1}. \tag{5.24}$$

In designing the parameters of the controller, compare the denominator of the transfer function with Butterworth Polynomial. The Butterworth polynomial for the third order is as follows

$$p^3 + 2p^2 w_0 + 2pw_0^2 + w_0^3 = 0. \tag{5.25}$$

Hence by comparing the denominator of the transfer function with above polynomial we get

$$k_p = \frac{w_0}{\cos\phi_1} \quad ; \quad k_i = \frac{2w_0^2 - \omega^2}{2\cos\phi_1}; \; w_0 = (2\cos\phi_1\omega^2 k_p - 2k_i\omega\sin\phi_1)^{1/3}.$$

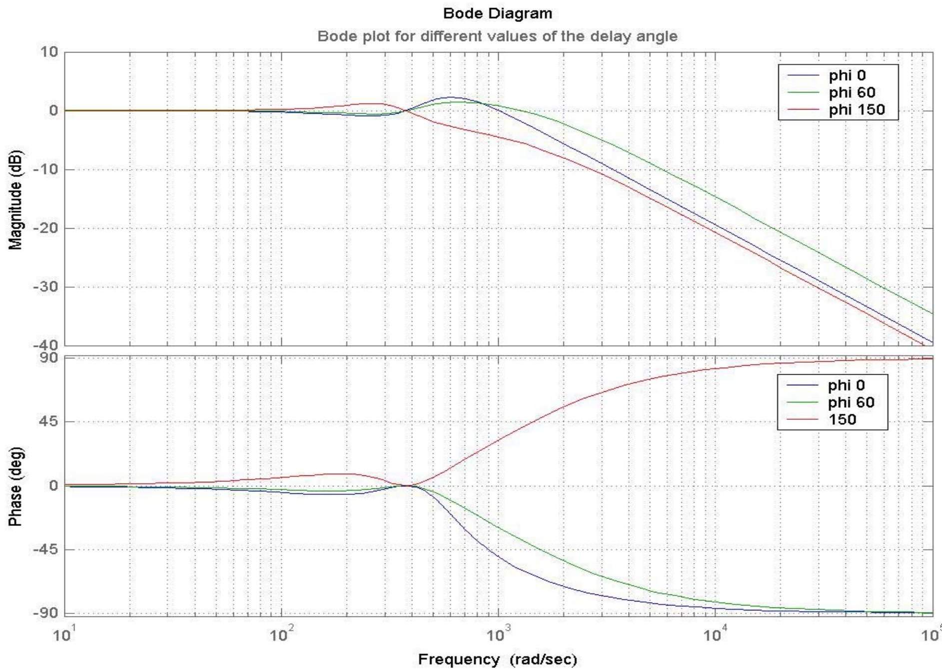

I

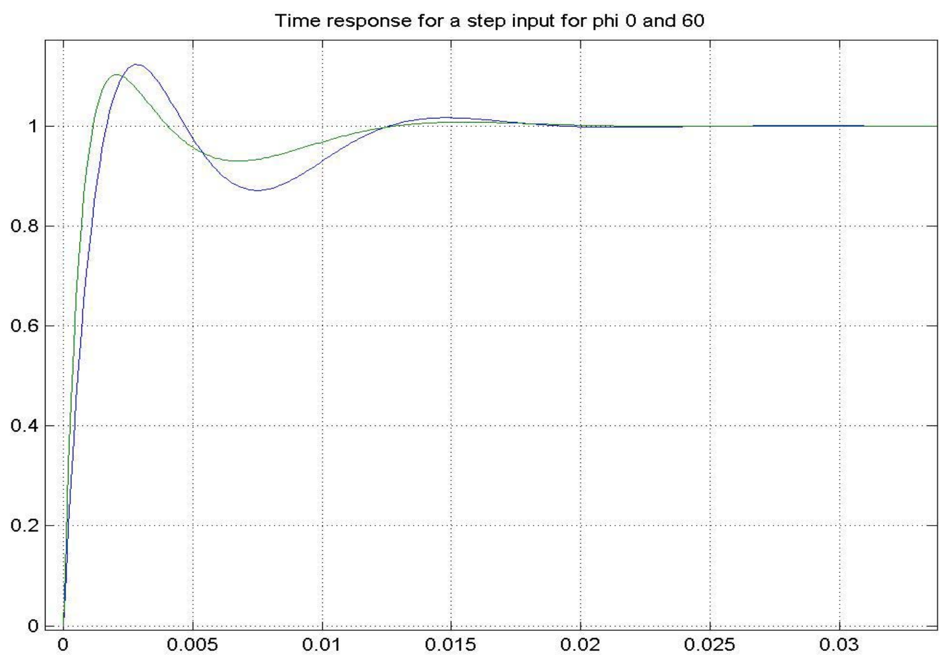

II

Figure 5.4: I. Effect of the delay angle I. Bode plot (magnitude and phase plots) II. Time response of the system

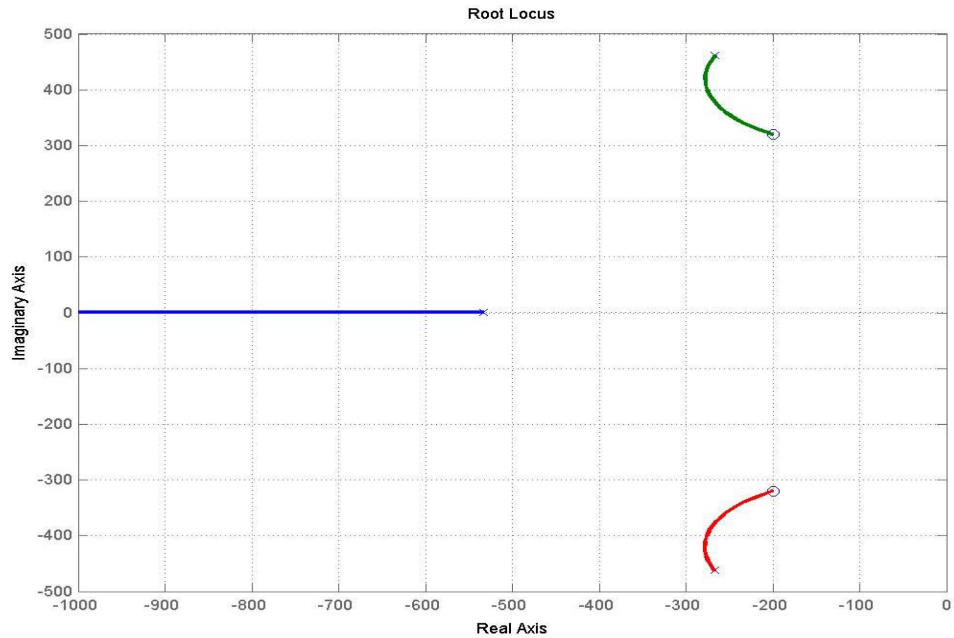

I

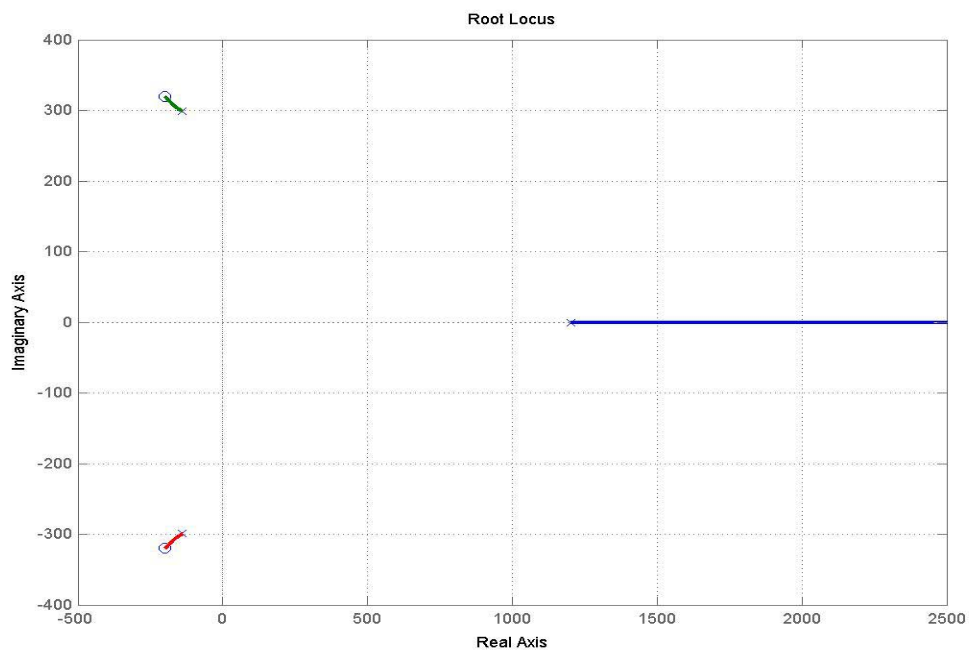

II

Figure 5.5: I. Effect of the delay angle I. Root locus of the system for angle 60^0 II. Root locus of the system for angle 150^0.

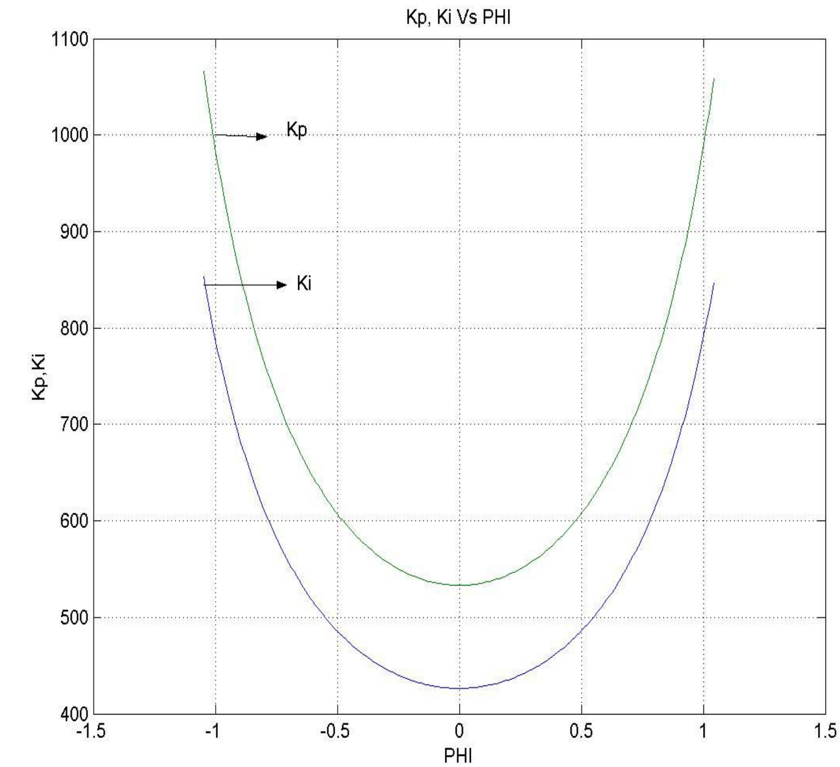

I

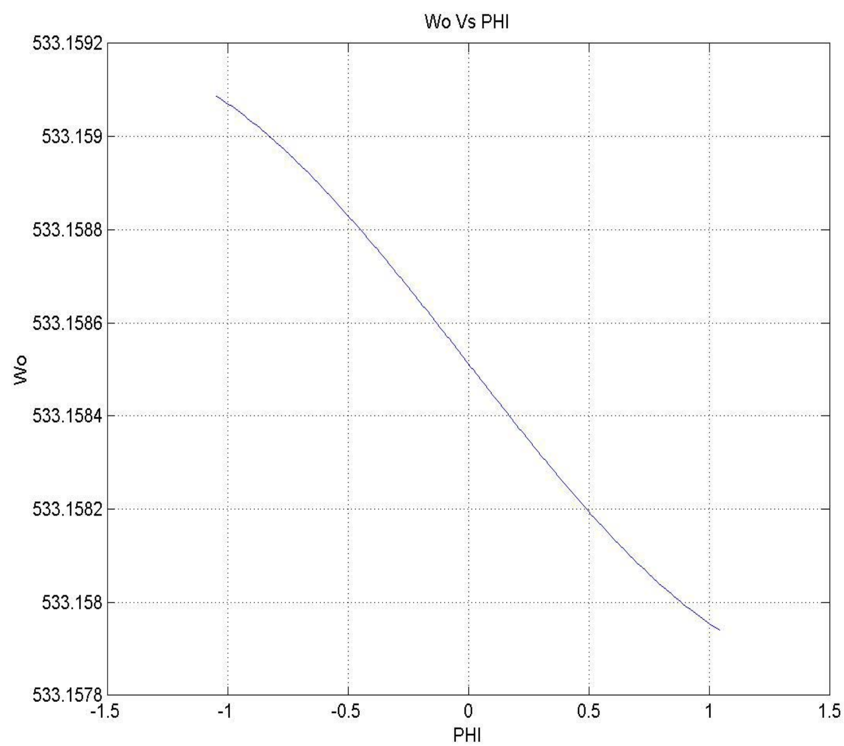

II

Figure 5.6 Effect of the delay angle I. Variation of the controller parameters K_p, K_i II. ω_0

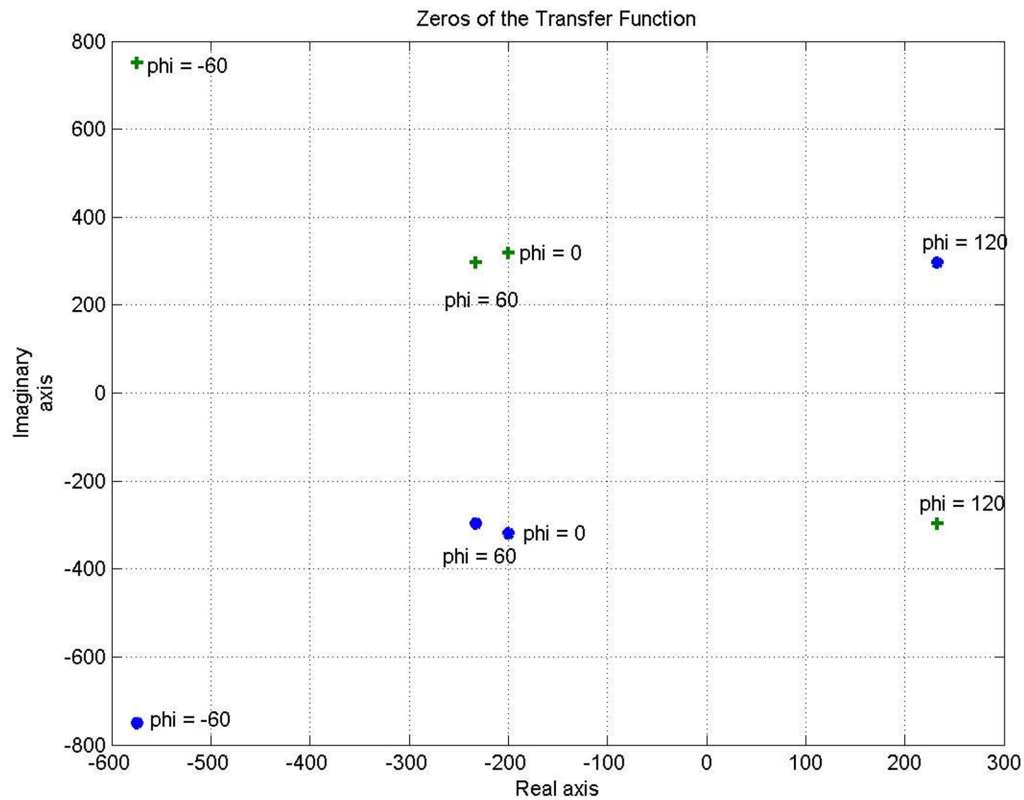

Figure 5.7: Effect of the delay angle on the zeros of the transfer function.

5.3.2 Effect of the Delay Angle

Figure 5.4 shows the bode plot of the transfer function for different values of the delay angle. The range of the delay angle is [-pi / 2, pi / 2] and beyond the angle ranges the system become unstable. As seen from Figure 5.4 (I), the phase angle plot, it can be observed that the phase margin becomes negative and which is a situation for instability. Also from the plots, the amount of phase angle added by different delay angles can be observed. Figure 5.4 (II) shows the time response of the system and the effect of the delay angle.

Figure 5.5 shows the root locus of the transfer function and it can be seen for delay angle of 150^0 the poles of the system lie on the right half of the plane i.e., the system is unstable. For the delay angle 60^0 the poles of the system are on the left half and these poles shift their position with delay angle and hence by varying the delay angle the control characteristics of the system can be changed. Figure 5.6 shows the variation of the control parameters with the variation in the delay angle. The parameter K_i is scaled down by a factor of 5000 and plotted. Hence choosing any particular point as the operating point, the transfer function of the controller is determined and used to control the variables. Figure 5.7 shows the placement of the zeros of the system with the variation of the delay angle. The zeros of the system are obtained by solving the numerator of the transfer function and these zeros determine the bandwidth of the controller. From Figure 5.7 it can be seen that for delay angle of 120^0, the zeros of the system are on the right half of the plane, which signifies that the system is unstable. Hence the choice of the delay angle determines the bandwidth and the stability of the system.

5.3.3 Transfer Function of the Controller

To find the transfer function of the controller $G_{AC}(s)$, from Figure 5.3

$$G_{AC}(s) = \frac{pi_a}{i_a^* - i_a}.$$

From Figure 5.3

$$\frac{pi_a}{i_a^* - i_a} = [e^{i\phi_1} K_p (p - j\omega) + e^{-i\phi_1} K_n (p + j\omega)]. \tag{5.26}$$

Let

$$K_p(p) = k_p + \frac{k_{ip}}{p}$$
$$K_n(p) = k_n + \frac{k_{in}}{p} \quad .$$

Hence by substituting the transfer functions of the PI controllers and assuming $k_{ip} = k_{in} = k_i ; k_n = k_p = k_p$ and simplifying

$$G_{AC}(s) = \frac{pI_a}{I_a^* - I_a} = \frac{p^2 2k_p \cos\phi_1 + p2k_i \cos\phi_1 + 2k_p \cos\phi_1 \omega^2}{p^2 + \omega^2} . \tag{5.27}$$

The k_p and k_i values are obtained as explained above and therefore the controller is used to control the current.

5.4 Generation of the Modulation Signals

Now that the output of the controllers is known; i.e., pI_a , pI_b and the third signal pI_c is obtained from the balance current equation. From (5.11) and Figure 5.1,

$$v_{an} = i_a R_a + L_a \sigma_a + e_a \tag{5.28}$$

$$v_{bn} = i_b R_b + L_b \sigma_b + e_b \tag{5.29}$$

$$v_{cn} = i_c R_c + L_c \sigma_c + e_c . \tag{5.30}$$

Also,

$$v_{aN} = v_{an} + V_{nN} \tag{5.31}$$

$$v_{bN} = v_{bn} + V_{nN} \tag{5.32}$$

$$v_{cN} = v_{cn} + V_{nN} . \tag{5.33}$$

where v_{aN}, v_{bN}, and v_{cN} are the output voltages of the inverter.

$$\frac{V_{dc}}{2}(2S_{ap}-1)=i_aR_a+L_api_a+e_a+V_{nN} \tag{5.34}$$

$$\frac{V_{dc}}{2}(2S_{bp}-1)=i_bR_b+L_bpi_b+e_b+V_{nN} \tag{5.35}$$

$$\frac{V_{dc}}{2}(2S_{cp}-1)=i_cR_c+L_cpi_c+e_c+V_{nN}\,. \tag{5.36}$$

The switching function can be expressed approximately as a function of the modulation signals such that

$$S_{ap}=\frac{1+m_{ap}}{2}$$

$$\Rightarrow m_{ap}=2S_{ap}-1.$$

Similarly

$$m_{bp}=2S_{bp}-1$$

$$m_{cp}=2S_{cp}-1.$$

Hence the modulation signals are given by

$$m_{ap}=\frac{v_{an}+V_{nN}}{V_d/2} \tag{5.37}$$

$$m_{bp}=\frac{v_{bn}+V_{nN}}{V_d/2} \tag{5.38}$$

$$m_{cp}=\frac{v_{cn}+V_{nN}}{V_d/2}\,. \tag{5.39}$$

Where v_{an}, v_{bn}, and v_{cn} are obtained from Equation (5.28).

5.5 Continuous PWM for Unbalanced Load Voltages

The expressions for the three modulation signals M_{ip} (I = abc) from (5.37-5.39) must be determined by the given phase voltages, which are not balanced in general. There are three linear independent equations to be solved to determine expressions for three unknown modulation signals and V_{nN}. These equations are under-determined. In view of this indeterminacy, there is an infinite number of solutions which are obtained by various optimizing performance functions defined in terms of the modulation functions. For a set of linear indeterminate equations expressed as AX = Y, a solution which minimizes the sum of squares of the variable X is obtained using the Moore-Penrose inverse [84]. The solution is given as $X = A^T[AA^T]^{-1}Y$. The solution is for the minimization of the sum of the squares of the equally weighted three modulation signals and the square of the normalized neutral voltage ($V^*_{nN} = 2V_{nN}/V_d$). Equivalently, this is the maximization of the inverter output-input voltage gain, i.e., $M_{ap}{}^2 + M_{bp}{}^2 + M_{cp}{}^2 + V^*_{nN}{}^2$ subject to the constraints in (5.1-5.3). The resulting expressions for the modulation signals are given as

$$m_{ap} = \frac{1}{2*V_d}(3*v_{an} - v_{bn} - v_{cn}); \tag{5.40}$$

$$m_{bp} = \frac{1}{2*V_d}(3*v_{bn} - v_{cn} - v_{an}); \tag{5.41}$$

$$m_{cp} = \frac{1}{2*V_d}(3*v_{cn} - v_{bn} - v_{an}); \tag{5.42}$$

$$V_{nN} = \frac{1}{2*V_d}(-v_{an} - v_{bn} - v_{cn}) \quad . \tag{5.43}$$

5.6 Discontinuous PWM for Unbalanced Voltages

An alternative carrier-based discontinuous modulation scheme is obtained by using the space vector methodology to determine the expression for V_{nN} in (5.31-5.33). For the unbalanced voltage set, the reference three-phase voltages mapped unto the stationary reference frame (V_{qdpn}) has in addition to the qp and dp voltage components, the nonzero, zero sequence voltage, V_{op}. This reference voltage is approximated by the time-average over a sampling period (converter switching period, T_s) of the two adjacent active states (V_{qdpna} , V_{qdpnb}) and the two zero states (V_{qdpn0}, V_{qdpn7}) . The expressions for the reference average neutral voltage, time-averaging the neutral voltages of the two active also approximates V_{nN} and two null modes as expressed in (5.46).

The turn-on and turn-off sequences of any of the switching transistors of the three-phase voltage source inverter shown in Figure 5.1 are represented by an existence function, which has a value of unity when it is turned on and becomes zero when it is turned off. In general, an existence function of a two-level converter is represented by $\mathbf{S_{ij}}$, i = a,b,c, and j = p, n, where i represents the load phase to which the device is connected, and j signifies top (p) and bottom (n) device of an inverter leg. Hence $\mathbf{S_{ap}}$, $\mathbf{S_{an}}$ which take values of zero or unity are, respectively, the existence functions of the top device ($\mathbf{T_{ap}}$) and bottom device ($\mathbf{T_{an}}$) of the inverter leg which are connected to phase 'a' load. In order to prevent short-circuiting the inverter DC source and thereby inviolate the Kirchoff's voltage law, $\mathbf{T_{ip}}$ and $\mathbf{T_{in}}$ cannot be turned on at the same time. Kirchoff's voltage law constraints the existence functions such that $\mathbf{S_{ip}} + \mathbf{S_{in}} = 1$, hence :

$$0.5\ V_d\ (2S_{ap} - 1) = v_{an} + V_{nN} \cong 0.5\ V_d\, M_{ap} \qquad (5.44)$$

$$0.5\ V_d\ (2S_{bp} - 1) = v_{bn} + V_{nN} \cong 0.5\ V_d\, M_{bp} \tag{5.45}$$

$$0.5\ V_d\,(2S_{cp} - 1) = v_{cn} + V_{nN} \cong 0.5\ V_d\, M_{cp}. \tag{5.46}$$

In Equations (5.44-5.46), V_{an}, $V_{bn,}$ V_{cn} are the phase voltages of the load while the voltage of the load neutral to inverter reference is V_{nN}. The voltage equations expressed in terms of the modulation signals in (5.44-5.46) are facilitated by the Fourier series approximation of the existence functions, which are approximated as

$$S_{ap} \cong 0.5\ (1 + M_{ap}), \quad S_{bp} \cong 0.5\ (1 + M_{bp}), \; S_{cp} \cong 0.5\ (1+M_{cp}) \tag{5.47}$$

where M_{ap} , M_{bp}, M_{cp} which range between –1 and 1 (for the linear modulation range) are the carrier-based modulation waveforms comprising of fundamental frequency components. In general, the actual existence functions are usually generated by comparing the high frequency triangle waveform, which ranges between –1 and 1 with the modulation waveforms (M_{ap}, M_{bp}, M_{cp}). The equations for the modulating signals of the top devices from (5.44-5.46) are expressed as

$$M_{ip} = 2v_{in}/V_d + 2V_{nN}/V_d \qquad\qquad i = a, b, c. \tag{5.48}$$

Table 5.1: Switching modes of the three-phase voltage source inverter and corresponding stationary reference frame qdpn voltages.

Mode	S_{ap}	S_{bp}	S_{cp}	V_{qs}	V_{ds}	V_{os}
U_0	0	0	0	0	0	$-V_d/2$
U_1	0	0	1	$-V_d/\sqrt{3}$	$V_d/\sqrt{3}$	$-V_d/6$
U_2	0	1	0	$-V_d/3$	$-V_d/\sqrt{3}$	$-V_d/6$
U_3	0	1	1	$-2V_d/3$	0	$V_d/6$
U_4	1	0	0	$2V_d/3$	0	$-V_d/6$
U_5	1	0	1	$V_d/3$	$-V_d/\sqrt{3}$	$V_d/6$
U_6	1	1	0	$V_d/3$	$V_d/\sqrt{3}$	$V_d/6$
U_7	1	1	1	0	0	$V_d/2$

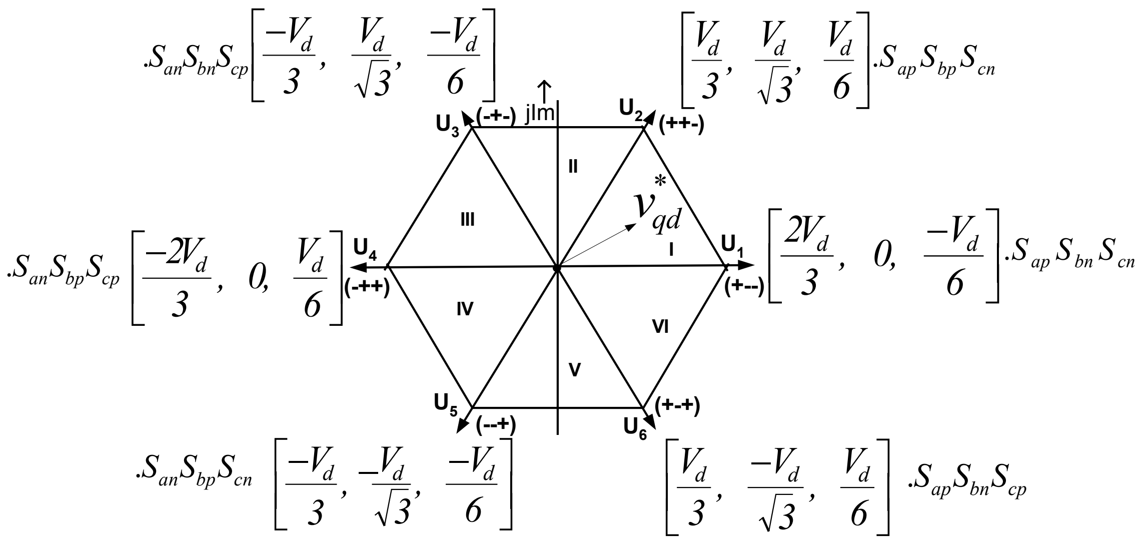

Figure 5.8: Voltage Space Vector diagram including zero sequence voltages.

The average neutral voltage, V_{nN} is determined using the method of space vector modulation. The eight feasible switching modes for the three-phase voltage source inverter are enumerated in Table 5.1.

The stationary reference frame qd and neutral voltages of the switching modes given in Figure 5.4 are expressed in the complex variable form as ($a = e^{j\varsigma}$, $\varsigma = 120°$) :

$$V_{qdp} = 2/3(v_{an} + a\, v_{bn} + a^2 v_{cn}), \quad V_{qp} = V_d/3(2S_{ap} - S_{bp} - S_{cp}), \quad \sqrt{3}V_{dp} = S_{cp} - S_{bp}$$

$$V_{pn} = V_{op} + V_d/3(S_{ap} + S_{bp} + S_{cp}) - V_d/2, \quad V_{op} = -1/3(v_{an} + v_{bn} + v_{cn}). \tag{5.49}$$

Note that V_{op} is equal to zero only when the reference voltage set is balanced. In general, the three-phase voltages expressed in the stationary reference frame ($V_{qdpn}^* \Rightarrow V_{qp}^*$, V_{dp}^*, V_{pn}^*) situated in the appropriate sector in Figure 5.8 are approximated by the time-average over a sampling period (converter switching period, T_s), of the two adjacent active voltage inverter vectors and the two zero states U_0 and U_7. The switching turn-on times of the two active and two null states are utilized to determine the duty cycle information to program the active switch gate signals. When the inverter is operating in the linear modulation region, the sum of the times the two active switching modes are utilized is less than the switching period; in which case the remaining time is occupied by using the two null vectors, U_0 and U_7. If the four voltage vectors V_{qdpna} , V_{qdpnb}, V_{qdpn0}, V_{qdpn7} are called into play for times t_a , t_b, t_0, t_7 (normalized with respect to modulator sampling time or converter switching period, T_s), respectively, then the qp and dp components of the reference voltage V_{qdp}^* are approximated as

$$V_{qdp}^* = V_{qp}^* + j\, V_{dp}^* = V_{qdpa}t_a + V_{qdpb}t_b + V_{qdp0}t_0 + V_{qdp7}t_7 \,,\ t_c = t_0 + t_7 = 1 - t_a - t_b. \tag{5.50}$$

When separated into real and imaginary parts, (1.44) gives the expressions for t_a and t_b as

$$t_a = \nabla\, [V_{qp}^* V_{dpb} - V_{dp}^* V_{qpb}], \quad t_b = \nabla\, [V_{dp}^* V_{qpa} - V_{qp}^* V_{dpa}] \,,\ \nabla = [\, V_{dpb} V_{qpa} - V_{qpb} V_{dpa}]^{-1}. \tag{5.51}$$

It is observed that both V_{qdp0} and V_{qdp7} do not influence the values of t_a and t_b .The times t_a and t_b expressed in terms of the instantaneous line-line reference voltages are given in Table 5.2 for the six sectors.

The neutral voltage V_{nN} averaged over the switching period Ts is given as

$$\langle V_{nN} \rangle = V_{oa}t_a + V_{ob}\, t_b + V_{o0}\, t_0 + V_{o7}\, t_7 - V_{op}. \tag{5.52}$$

It should be noted that t_c is partitioned into dwell times for the two null voltage vector - $t_c\alpha$ for U_o and $t_c(1-\alpha)$ for U_7. The averaged neutral voltages for reference voltages in the voltage sectors calculated using (5.52) are shown in Table 5.3.

Table 5.2: Device switching times expressed in terms of reference line-line voltages

Sector	I	II	III	IV	V	VI
$V_d\, t_a$	v_{ac}	v_{ab}	v_{cb}	v_{ca}	v_{ba}	v_{bc}
$V_d\, t_b$	v_{cb}	v_{ca}	v_{ba}	v_{bc}	v_{ac}	v_{ab}
Max voltage	v_{ap}	v_{bp}	v_{bp}	v_{cp}	v_{cp}	v_{ap}
Min Voltage	v_{cp}	v_{cp}	v_{ap}	v_{ap}	v_{bp}	v_{bp}

Table 5.3 gives the expression for the averaged neutral voltage $<V_{nN}>$ for the six sectors of the space vector. Hence, given the unbalanced voltage set at any instant, V^*_{qdo} in the stationary reference frame is found and the sector in which V_{qd}^* is located is determined. The expression for V_{nN} is then selected and is subsequently used in (5.37-5.39) to determine the modulation signals for the three top devices.

Hence, given the unbalanced voltage set at any instant, V^*_{qdp} in the stationary reference frame is found and the sector (Table 5.3) in which it is located is determined.

Table 5.3: Expressions for the neutral voltage for the six sectors

Sector	Neutral Voltage $<V_{nN}>$
VI	$(2v_{bn} - v_{an} - v_{cn})/6 + 0.5V_d\,(1\text{-}2\alpha) + 0.5\,(1\text{-}2\alpha)[v_{cn} - v_{an}]$
V	$(2v_{an} - v_{bn} - v_{cn})/6 + 0.5V_d\,(1\text{-}2\alpha) + 0.5\,(1\text{-}2\alpha)[v_{cn} - v_{bn}]$
IV	$(2v_{cn} - v_{an} - v_{bn})/6 + 0.5V_d(1\text{-}2\alpha) + 0.5\,(1\text{-}2\alpha)[v_{an} - v_{bn}]$
III	$(2v_{bn} - v_{an} - v_{cn})/6 + 0.5\,V_d(1\text{-}2\alpha) + 0.5\,(1\text{-}2\alpha)[v_{an} - v_{cn}]$
II	$(2v_{an} - v_{bn} - v_{cn})/6 + 0.5V_d\,(1\text{-}2\alpha) + 0.5\,(1\text{-}2\alpha)[v_{bn} - v_{n}]$
I	$(2v_{n} - v_{n} - v_{n})/6 + 0.5\,V_d(1\text{-}2\alpha) + 0.5\,(1\text{-}2\alpha)[v_{n} - v_{n}]$

The corresponding expression for V_{nN} is then selected from Table 5.1 and is subsequently used in (5.37-5.39) to determine the modulation signals for the three top devices.

5.7 Generalized Discontinuous Carrier-based PWM Scheme for Balanced and Unbalanced Voltage Source Inverter

This section of the chapter presents the unified theory for the discontinuous carrier-based PWM methodology for balanced and unbalanced voltage source inverter while retaining the benefits of the generalized discontinuous modulation. This scheme eliminates the computational burden that is being caused in case of the unbalanced situation, which was observed in the above methodology; i.e., in case of the unbalanced situation, the zero sequence voltage V_{nN} has to be calculated in each of the sectors as the magnitude varies depending on where the reference vector lies. The different expression of the zero sequence voltage is tabulated in Table 5.3. In the present case a generalized zero sequence voltage expression is being derived which is applicable for both the balanced and unbalanced conditions.

Under balanced conditions three-phase reference voltage set, Table 5.4, the average neutral voltage expressions for the six sectors unifies to Eq. (5.47)

$$< V_{nN} >= 0.5(1-2\alpha)-\alpha v_{\min} + v_{\max}(\alpha-1). \qquad (5.47)$$

When the zero sequence component of the voltage is removed from each of the three-phase unbalanced fundamental voltages, the resulting set of three-phase signals is

Table 5.4: Device Switching times expressed in terms of reference line-line Voltages

Sector	I	II	III	IV	V	VI
$V_d\ t_a$	v_{ac}	v_{ab}	v_{cb}	v_{ca}	v_{ba}	v_{bc}
$V_d\ t_b$	v_{cb}	v_{ca}	v_{ba}	v_{bc}	v_{ac}	v_{ab}
Max voltage	$v_{ap} - V_{nN}$	$v_{bp} - V_{nN}$	$v_{bp} - V_{nN}$	$v_{cp} - V_{nN}$	$v_{cp} - V_{nN}$	$v_{ap} - V_{nN}$
Min Voltage	$v_{cp} - V_{nN}$	$v_{cp} - V_{nN}$	$v_{ap} - V_{nN}$	$v_{ap} - V_{nN}$	$v_{bp} - V_{nN}$	$v_{bp} - V_{nN}$

balanced with 120^0 symmetry. This property makes it possible to locate the sectors of qd components of unbalanced voltage as shown in Table 5.5. Hence if the unbalanced phase voltages are instantaneously diminished by the value of the zero sequence voltage, the modified phase voltages are balanced and can be used to generalize Table 5.4 to give the average neutral voltage as

$$< V_{nN} >= 0.5(1-2\alpha) - \alpha v_{\min}{}' + v_{\max}{}'(\alpha - 1). \tag{5.48}$$

where $v_{min}' =$ Minimum (v_{an}', v_{bn}', v_{cn}'), $v_{man}' =$ Maximum (v_{an}', v_{bn}', v_{cn}')

and $v_{in}' = v_{in} - V_{nN}$ $i = a, b, c$.

Hence using the above generalized zero sequence voltage expression the discontinuous modulation can be implemented. Hence the approach makes the implementation of the unbalanced system easy without any complex computations to calculate the turn on times of the devices. Also there is no need of search to find the combination of the switch mode and the subsequent sequencing of switching vectors.

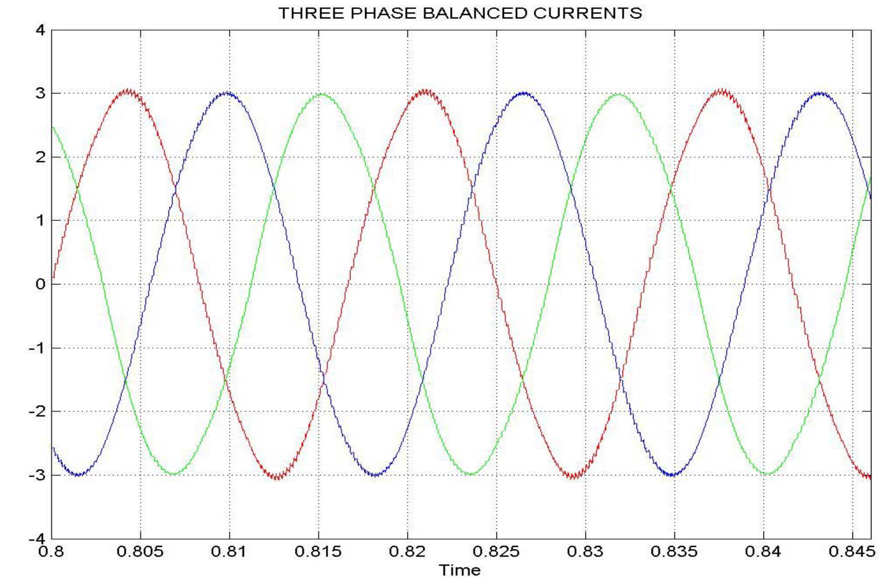

I

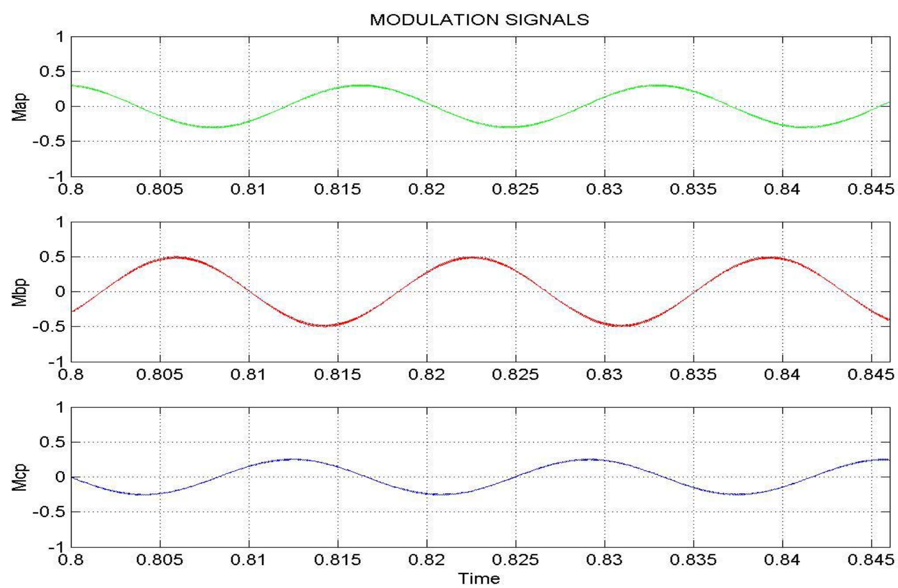

(a)

(b)

(c)

II

Figure 5.9: Continuous modulation I. Three phase balanced currents II. Three phase modulation signals.

(a)
(b)
(c)

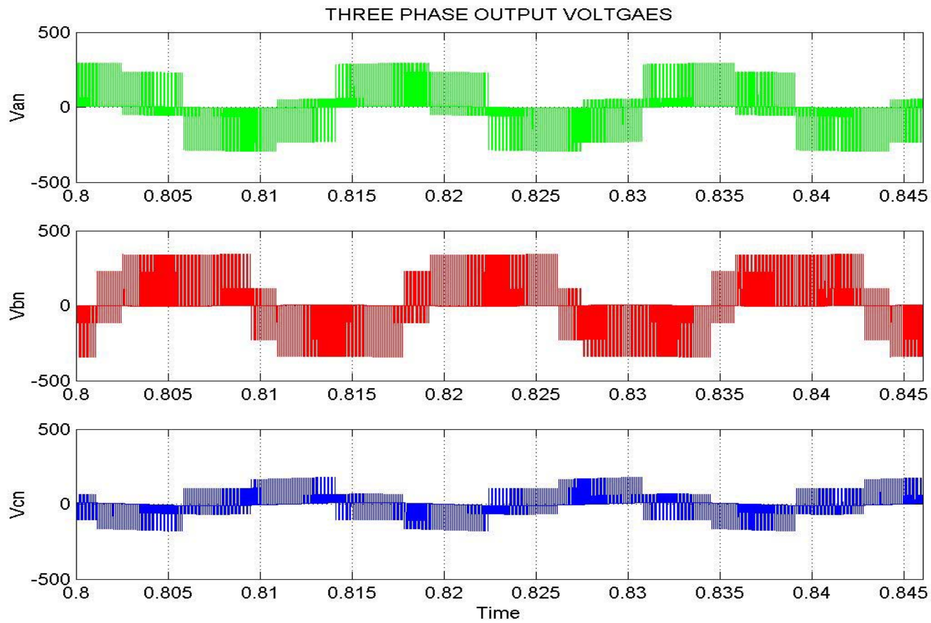

I

(a)
(b)

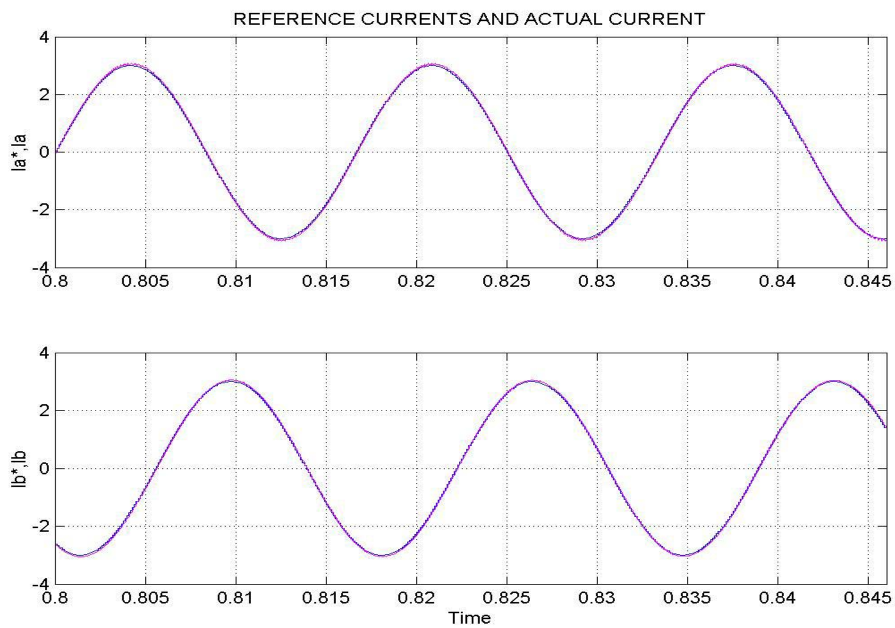

II

(d)

Figure 5.10: Continuous modulation: I (a) (b) (c) Three phase voltages II. (a) (b)Tracking of the reference currents by the controller

(a)
(b)
(c)

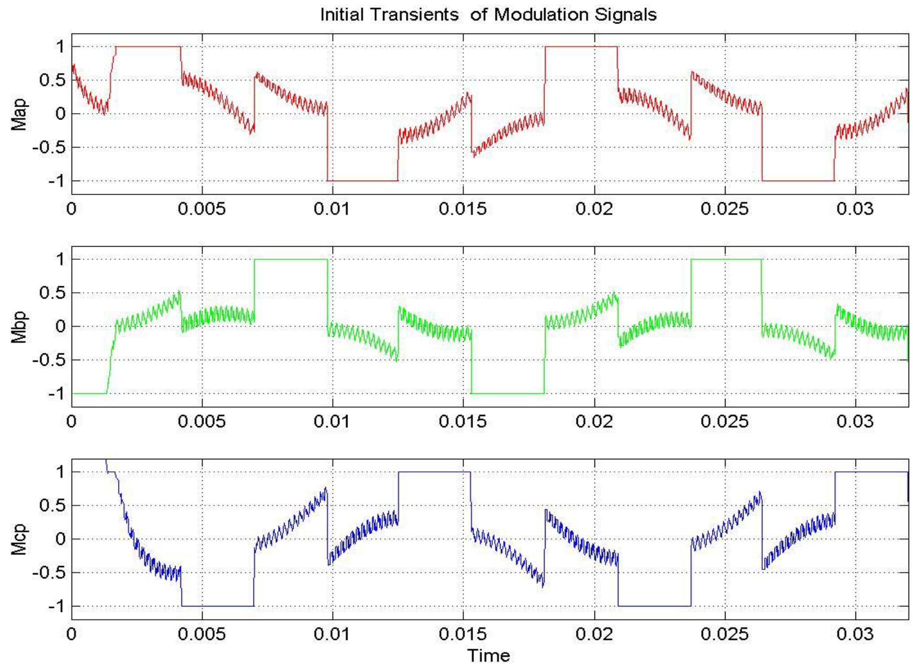

I

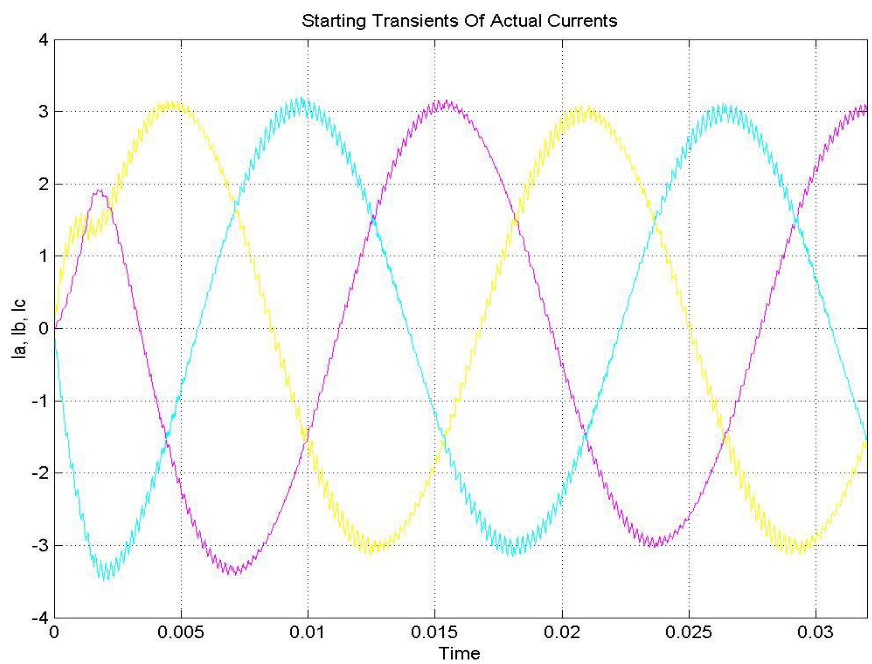

II

Figure 5.11: Discontinuous modulation for $\delta = -\frac{\pi}{3}$, initial transients of the system. I. Three phase modulation signals II. Three phase-balanced currents.

(a)

(b)

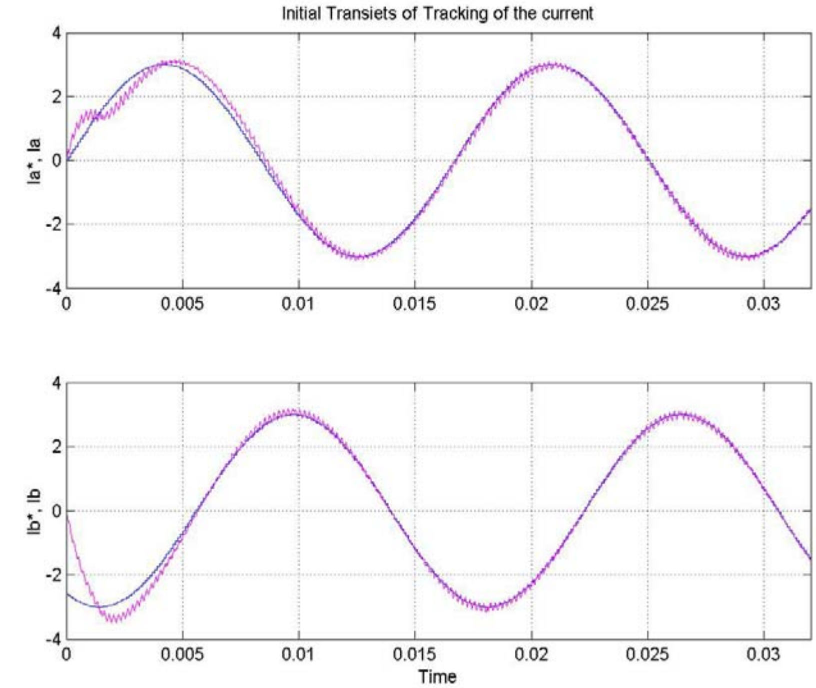

I

(a)

(b)

(c)

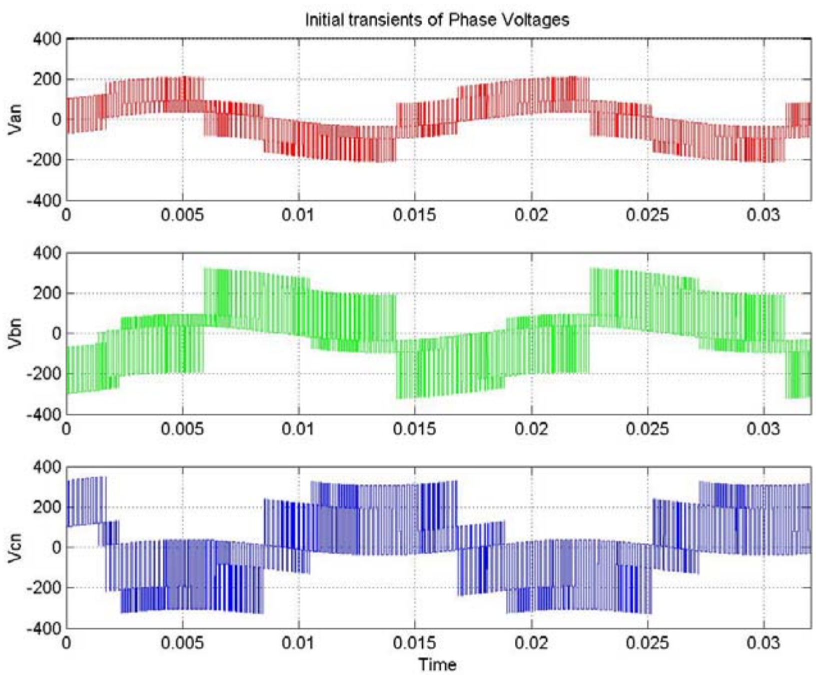

II

Figure 5.12: Discontinuous modulation for $\delta = -\frac{\pi}{3}$, initial transients of the system. I. (a) (b) Tracking of the reference currents II. (a) ,(b), (c) Three-phase voltages.

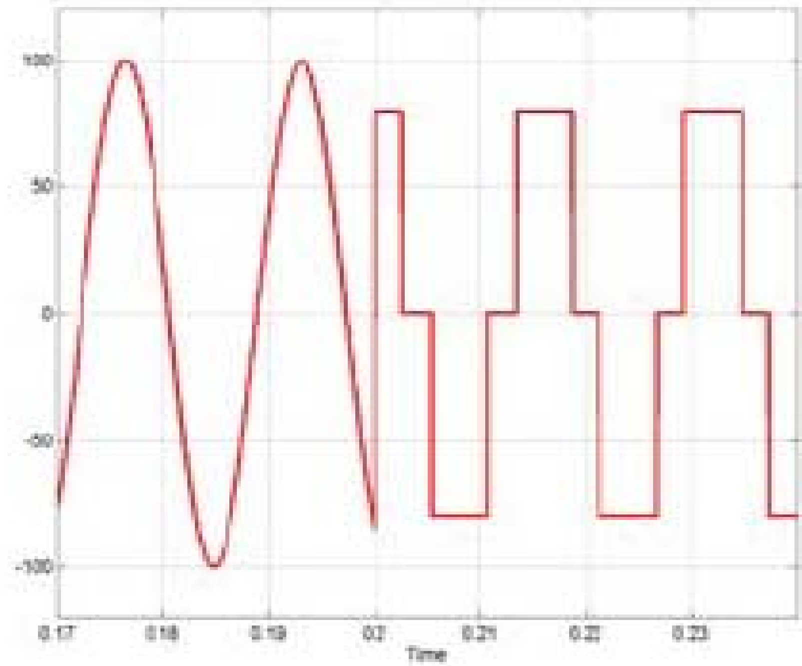

I

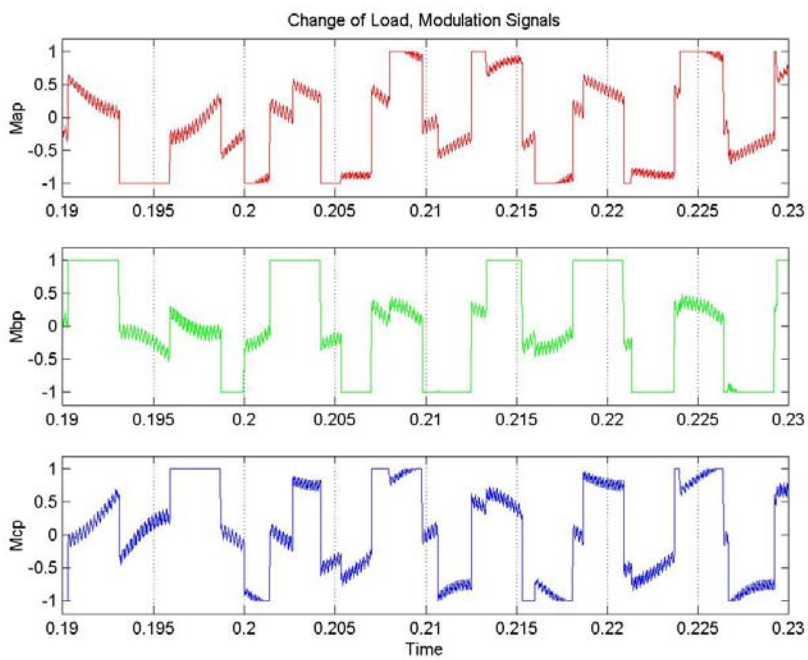

(a)

(b)

(c)

II

Figure 5.13: Discontinuous modulation for $\delta = -\frac{\pi}{3}$, transients of the system during the load change. I. Change of back-emf from sine to a square wave. II. Three phase modulation signals.

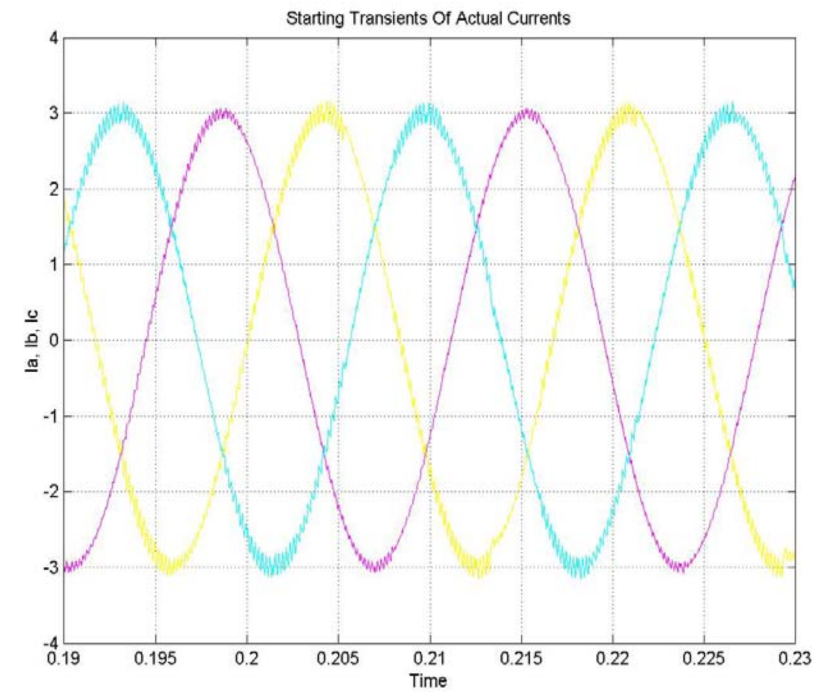

I

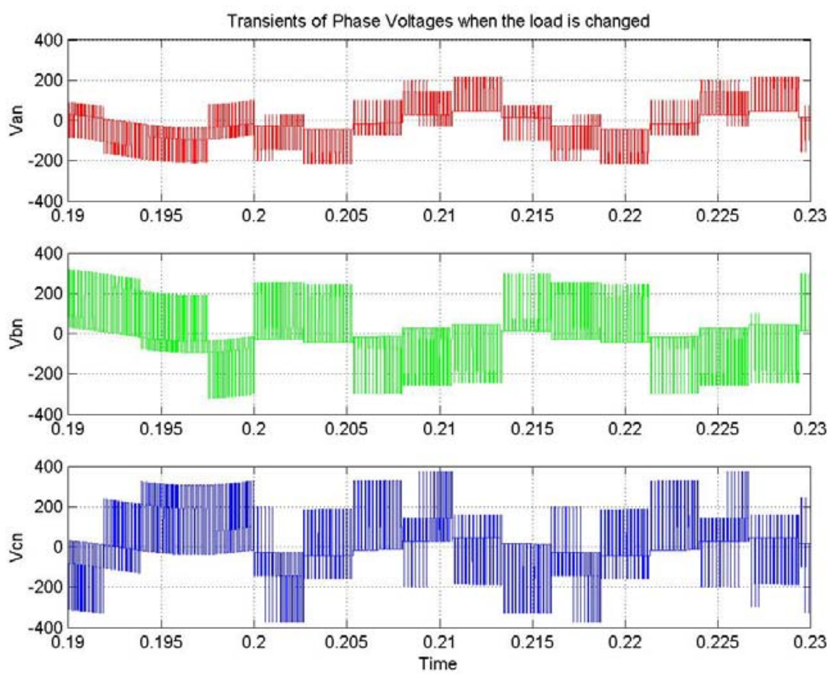

(a)

(b)

(c)

II

Figure 5.14: Discontinuous modulation for $\delta = -\frac{\pi}{3}$, transients of the system during the load change. I Three-phase balanced currents. II. Three-phase voltages.

5.8 Simulation Results

Figures 5.9 – 5.10 shows the simulation results for the control scheme using continuous modulation scheme. Figure 5.9 II shows the three phase modulation signals which when modulated using the carrier-based PWM generates the switching for the devices to produce the balanced phase currents. Figure 5.9 I show the balanced currents produced by the scheme. Figure 5.10 I show the unbalanced three phase voltages impressed across the load. Figure 5.10 II shows the reference current and the actual phase current on the same plot and hence it is clear that the phase currents so produced are balanced currents since the controller is tracking the assumed balanced currents. The load in the particular case is, for t = 0 sec to t = 1sec $R_a = 1\Omega$, $R_b = 3\Omega$, $R_c = 4\Omega$, $L_a = 0.025H$, $L_b = 0.05H$, $L_c = 0.1H$, $e_a = 100 \sin(\omega t)$, $e_b = 100 \sin(\omega t\text{-}120^o)$, and $e_c = 100 \sin(\omega t+120^o)$. The dc supply voltage used is in this case is $V_d = 400$ V.

In the discontinuous mode, assume $\delta = -60^o$. In this case $V_d = 200V$. Figures 5.11 – 5.12 illustrates the initial transients of the system. Figure 5.11 I shows the discontinuous modulation signals required to generate the balanced currents and as seen from the figure the devices will be clamped to the negative and the positive dc rails for 120^0 and depending on the unbalance the clamping period will shift in the cycle. Figure 5.11 II show the three phase balanced currents generated. Figure 5.12 I shows the three phase unbalanced voltages impressed across the load and the Figure 5.12 II shows the effectiveness of the controller to track the reference currents. After reaching the steady state the back-emf connected as the load is changed from the sine wave to a square wave to create the extreme unbalance condition. The change in load occurs at t = 0.2 sec. The magnitude of the square is 50 V. Even under this unbalanced condition the controller tracks the reference currents. Figures 5.13 – 5.14 shows the transients of the system during the change of the load.

5.8 Unbalance Operation of a Two-Level Three-Phase Rectifier

In recent years, there was a significant increase in the usage of the rectifiers in converting the power generated. Especially, diode and thyristor rectifiers are commonly applied in the front end of dc-link power converters as an interface with the ac power line. The rectifiers are nonlinear in nature and consequently generate harmonic currents in the ac power line. The high harmonic content of the line current and the resulting low power factor of the load cause a number of problems in the power distribution.

- Voltage distortion and electromagnetic interface affecting other users of the power system.
- Increase voltampere (VA) ratings of the power system equipment to handle the harmonics.

In real world, no system is balanced and hence the significance of the study of the unbalanced system increasing day-by-day. In the present section, the unbalance operation of the two-level rectifier is considered.

5.9 Circuit Configuration

The circuit configuration is based on the general three-phase two-level converter with unbalanced source and input impedances as shown in Figure 5.15. The converter consists of boost inductors L_a, L_b, and L_c on the ac side to filter out the input harmonic current and achieve sinusoidal current waveforms. R_a, R_b, and R_c are the series equivalent resistors. Six switching devices with a rating of V_{dc} are used.

Applying the KVL for the input side, the supply voltage can be written as the sum of the voltage drop across the input side impedance

$$v_a = i_a R_a + L_a p i_a + v_{ao} \tag{5.48}$$

$$v_b = i_b R_b + L_b p i_b + v_{bo} \tag{5.49}$$

$$v_c = i_c R_c + L_c p i_c + v_{co} . \tag{5.50}$$

The voltage v_{ao} is given by

$$v_{ao} = S_{ap} V_{kN} + S_{an} V_{No} \tag{5.51}$$

$$v_{ao} = S_{ap} V_{kN} + S_{an} V_{No} \tag{5.52}$$

$$v_{ao} = S_{ap} V_{kN} + S_{an} V_{No} . \tag{5.53}$$

To avoid shorting of the output capacitor the following constraint has to be followed while switching the devices.

$$S_{ap} + S_{an} = 1 \Rightarrow S_{ap} = 1 - S_{an} \tag{5.54}$$

$$S_{bp} + S_{bn} = 1 \Rightarrow S_{bp} = 1 - S_{bn} \tag{5.55}$$

$$S_{cp} + S_{cn} = 1 \Rightarrow S_{cp} = 1 - S_{cn} . \tag{5.56}$$

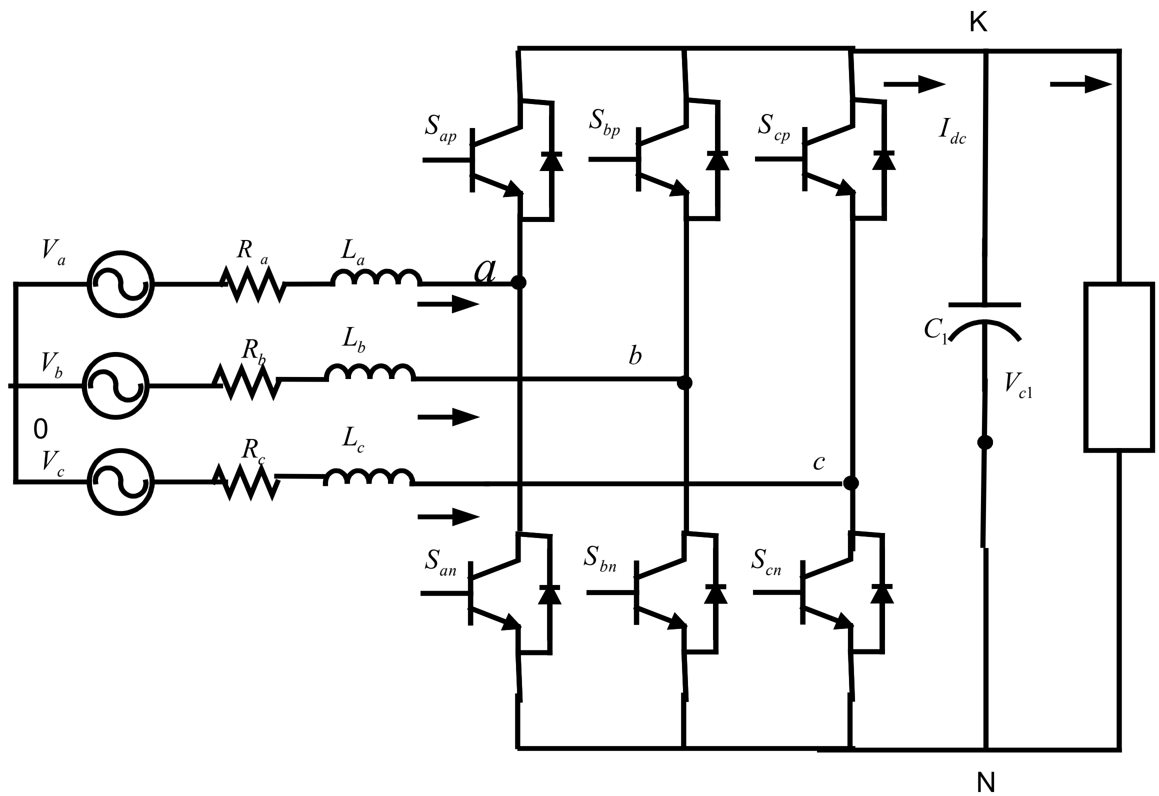

Figure 5.15: Schematic of the three-phase two-level rectifier.

Hence by substituting the expression in Eqs. (5.51-5.53) into Eqs. (5.48-5.50)

$$v_a = i_a R_a + L_a p i_a + \left(S_{ap} - S_{an}\right)\frac{V_{kN}}{2} + V_{N0} \tag{5.57}$$

$$v_b = i_b R_b + L_b p i_b + \left(S_{bp} - S_{bn}\right)\frac{V_{kN}}{2} + V_{N0} \tag{5.58}$$

$$v_c = i_c R_c + L_c p i_c + \left(S_{cp} - S_{cn}\right)\frac{V_{kN}}{2} + V_{N0}\,. \tag{5.59}$$

Hence

$$\left(S_{ap} - S_{an}\right) = \frac{v_a - i_a R_a - L_a p i_a - V_{N0}}{\dfrac{V_{kN}}{2}} \tag{5.60}$$

$$\left(S_{bp} - S_{bn}\right) = \frac{v_b - i_b R_b - L_b p i_b - V_{N0}}{\dfrac{V_{kN}}{2}} \tag{5.61}$$

$$\left(S_{cp} - S_{cn}\right) = \frac{v_c - i_c R_c - L_c p i_c - V_{N0}}{\frac{V_{kN}}{2}}. \tag{5.62}$$

The relationship between the switching function and the modulation signals can be expressed as

$$S_{ap} = \frac{\left(1 + M_a\right)}{2} \tag{5.63}$$

$$S_{bp} = \frac{\left(1 + M_b\right)}{2} \tag{5.64}$$

$$S_{cp} = \frac{\left(1 + M_c\right)}{2}. \tag{5.65}$$

By substituting the conditions in Eqs. (5.63 – 5.65) and Eqs. (5.54 – 5.56) in Eqs. (5.60 – 5.62) gives the modulation signals as

$$M_{ap} = \frac{v_a - I_a R_a - L_a p I_a - V_{N0}}{V_{kN}} \tag{5.66}$$

$$M_{bp} = \frac{v_b - i_b R_b - L_b p i_b - V_{N0}}{V_{kN}} \tag{5.67}$$

$$M_{cp} = \frac{v_c - i_c R_c - L_c p i_c - V_{N0}}{V_{kN}}. \tag{5.68}$$

The current flowing through the capacitor is given by

$$C p V_d = -I_{dc} + \left(M_{ap} i_a + M_{bp} i_b + M_{cp} i_c\right). \tag{5.69}$$

5.10 Control Scheme

The control structure is as shown in Figure 5.16. As seen the structure is similar to that of the three-level rectifier. Similar control methodology is applied to derive the reference phase currents.

Now

$$i_a R_a + L_a p i_a = \sigma_a \tag{5.70}$$

$$i_b R_b + L_b p i_b = \sigma_b \tag{5.71}$$

$$i_c R_c + L_c p i_c = \sigma_c \,. \tag{5.72}$$

By substituting the above assumption in Eqs. (5.66 – 5.68) and simplifying, the expressions for the modulation signals are obtained as

$$M_{ap} = \frac{v_a - \sigma_a - V_{N0}}{V_{dc}} \tag{5.73}$$

$$M_{bp} = \frac{v_b - \sigma_b - V_{N0}}{V_{dc}} \tag{5.74}$$

$$M_{cp} = \frac{v_c - \sigma_c - V_{N0}}{V_{dc}} \,. \tag{5.75}$$

The capacitor equation is given by

$$CpV_{dc} = -I_{dc} + \left(M_{ap} i_a + M_{bp} i_b + M_{cp} i_c\right).$$

By substituting the expressions for the modulation signals and simplifying

$$\frac{1}{2} CpV_d^{\,2} + I_{dc} V_d = \left(v_{as}{}' i_a + v_{bs}{}' i_b + v_{cs}{}' i_c - \sigma_a i_a - \sigma_b i_b - \sigma_c i_c\right). \tag{5.76}$$

The power transferred in a three-phase circuit is given by

$$P = v_{as} i_a + v_{bs} i_b + v_{cs} i_c \,. \tag{5.77}$$

Under balanced conditions, the sum of the three phase currents is equal to zero

$$i_a + i_b + i_c = 0$$
$$\Rightarrow i_c = -(i_a + i_b) \; . \tag{5.78}$$

Substituting Eq. (5.78) in Eq. (5.77) gives

$$P = v_{ac} i_a + v_{bc} i_b \; . \tag{5.79}$$

The main objective of the control scheme is to transfer constant power and hence the differentiation of power with respect to time is zero; i.e.,

$$\frac{\partial P}{\partial t} = 0$$

$$\Rightarrow$$

$$0 = i_a p v_{ac} + v_{ac} p i_a + I_b p v_{bc} + v_{bc} p i_b \tag{5.80}$$

where $p = \dfrac{\partial}{\partial t}$.

From Eqs. (5.70 – 5.71), by substituting the expressions for pi_a and pi_b in Eq. (5.80) gives the condition for the constant power transfer

$$i_a \left[L_a L_b p v_{ac} - L_b R_a v_{ac} \right] + i_b \left[L_a L_b p v_{bc} - L_a R_b v_{ac} \right] = -\left[L_b v_{ac} \sigma_a + L_a v_{bc} \sigma_b \right]. \tag{5.81}$$

Expressing Eq. (5.76) and (5.81) in the matrix form

$$\begin{bmatrix} L_a L_b p v_{ac} - L_b R_a v_{ac} & L_a L_b p v_{bc} - L_a R_b v_{bc} \\ v_{ac} + \sigma_c - \sigma_a & v_{bc} + \sigma_c - \sigma_b \end{bmatrix} \begin{bmatrix} i_a \\ i_b \end{bmatrix} = \begin{bmatrix} -\left[L_b v_{ac} \sigma_a + L_a v_{bc} \sigma_b \right] \\ \sigma_v + I_{dc} \left(V_{c1} + V_{c2} \right) \end{bmatrix}.$$

By solving the above matrix for I_a, I_b

$$i_a = \frac{\left(v_{bc} + \sigma_c - \sigma_b\right)\left(-\left[L_b v_{ac}\sigma_a + L_a v_{bc}\sigma_b\right]\right) - \left(\sigma_v + I_{dc}\left(V_{c1} + V_{c2}\right)\right)\left(L_a L_b p v_{bc} - L_a R_b v_{bc}\right)}{\Delta} \tag{5.82}$$

$$i_b = \frac{\left(L_a L_b p v_{ac} - L_b R_a v_{ac}\right)\left(\sigma_v + I_{dc}\left(V_{c1} + V_{c2}\right)\right) - \left(v_{ac} + \sigma_c - \sigma_a\right)\left(-\left[L_b v_{ac}\sigma_a + L_a v_{bc}\sigma_b\right]\right)}{\Delta} \tag{5.83}$$

where

$$\Delta = \left(L_a L_b p v_{ac} - L_b R_a v_{ac}\right)\left(v_{bc} + \sigma_c - \sigma_b\right) - \left(L_a L_b p v_{bc} - L_a R_b v_{bc}\right)\left(v_{ac} + \sigma_c - \sigma_a\right).$$

Using the above expressions the reference phase currents can be generated. Phase c current can be obtained using the balance condition for the current.

Figure 5.16 shows the schematic of the control scheme. Similar to three level rectifier control scheme, two level rectifiers also have the voltage control as the outer control loop and the current controllers as the inner control loop. In the control scheme the square of the actual dc voltage $V_{dc}^{\;2}$ is compared with the square of the reference dc voltage $V_{dc}^{\;*2}$. The error signal is passed through a PI controller K_v whose structure is explained in the next section. The output of this controller is assumed as σ_v. Using σ_v, the expression for constant power and using Equations (5.82-5.83), the reference currents $i_a^{\;*}$, $i_b^{\;*}$, and $i_c^{\;*}$ can be calculated. These reference currents are compared with the actual currents. The errors are passed through the natural reference frame current controllers K_a, K_b, and K_c. The structure of these controllers is explained in the next section. The output of these controllers is assumed as σ_a, σ_b, and σ_c. Using Equations (5.73) -(5.75) the modulation signals can be obtained.

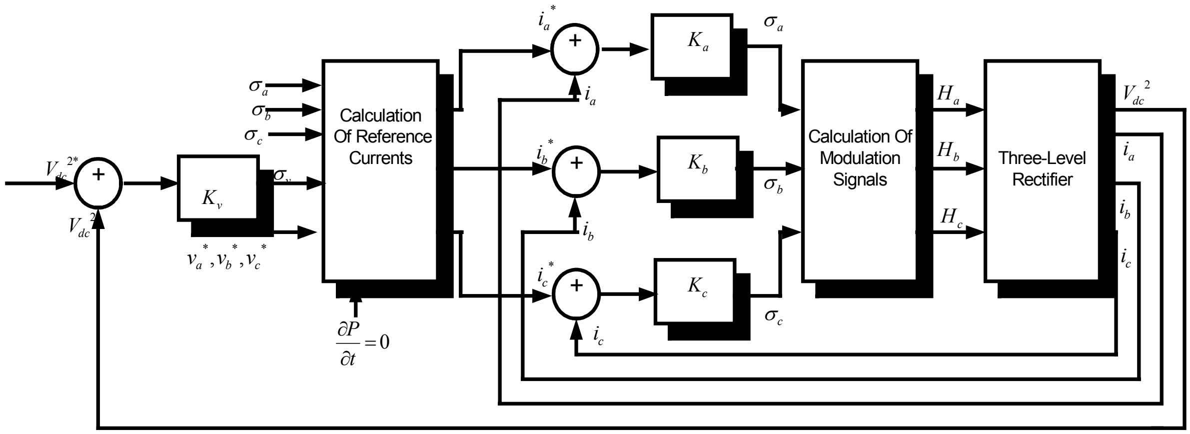

Figure 5.16: Schematic of the control scheme of two-level rectifier.

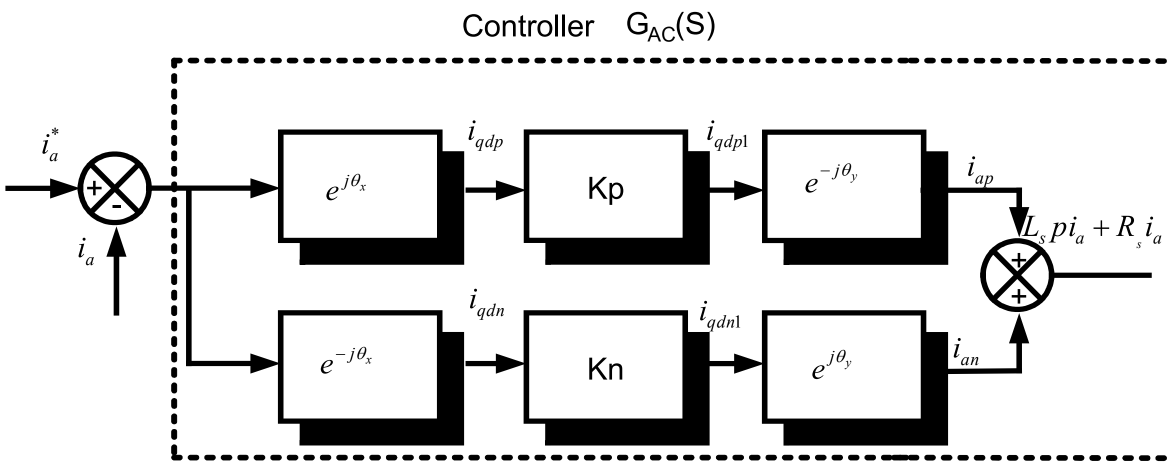

Figure 5.17: Structure of the abc reference frame controller.

5.10.1 Structure of the Controllers

The procedure for determining the transfer functions of the currents is discussed in section 5.3.1. Using the same methodology the transfer functions are derived as follows:

$$\frac{i_a}{i_a^*} = \frac{p^2 2K_p Cos\phi_1 + 2pK_i Cos\phi_1 + 2K_p Cos\phi_1 \omega^2 - 2K_i \omega Sin\phi_1}{L_a p^3 + p^2\left[R_a + 2K_p Cos\phi_1\right] + p\left[3\omega_s^2 L_a + 2K_i Cos\phi_1\right] + \left[R_a \omega_s^2 + 2K_p Cos\phi_1 \omega^2 - 2K_i \omega Sin\phi_1\right]}$$

$$\frac{i_b}{i_b^*} = \frac{p^2 2K_p Cos\phi_1 + 2pK_i Cos\phi_1 + 2K_p Cos\phi_1 \omega^2 - 2K_i \omega Sin\phi_1}{L_b p^3 + p^2\left[R_b + 2K_p Cos\phi_1\right] + p\left[3\omega_s^2 L_b + 2K_i Cos\phi_1\right] + \left[R_b \omega_s^2 + 2K_p Cos\phi_1 \omega^2 - 2K_i \omega Sin\phi_1\right]}$$

$$\frac{i_c}{i_c^*} = \frac{p^2 2K_p Cos\phi_1 + 2pK_i Cos\phi_1 + 2K_p Cos\phi_1 \omega^2 - 2K_i \omega Sin\phi_1}{L_c p^3 + p^2\left[R_c + 2K_p Cos\phi_1\right] + p\left[3\omega_s^2 L_c + 2K_i Cos\phi_1\right] + \left[R_c \omega_s^2 + 2K_p Cos\phi_1 \omega^2 - 2K_i \omega Sin\phi_1\right]}.$$

Comparing the denominator of the transfer function with the Butterworth polynomial is one of the useful techniques in choosing the controller parameters. As seen from the transfer functions, it is clear that the system is a third order system and hence by comparing the denominator with third order polynomial.

$$p^3 + 2p^2\omega_o + 2p\omega_o^2 + \omega_o^3 = 0. \tag{5.84}$$

Following equations are obtained

$$\frac{R_a + 2K_p Cos\phi_1}{L_a} = 2\omega_o \tag{5.85}$$

$$\frac{\omega_s^2 L_a + 2K_i Cos\phi_1}{L_a} = 2\omega_o^2 \tag{5.86}$$

$$\frac{R_a \omega_s^2 + 2K_p Cos\phi_1 \omega^2 - 2K_i \omega Sin\phi_1}{L_a} = \omega_o^3. \tag{5.87}$$

Solving the above equations and by varying the delay angle, the controller parameters of the current controller can be obtained.

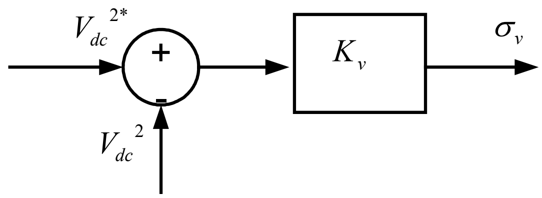

Figure 5.18: Structure of the voltage controller.

5.10.2 Voltage Controller

From Figure 5.18

$$\left(V_{dc}^{*2} - V_{dc}^{2}\right)K_v = \frac{1}{2} C p V_{dc}^{2}$$

$$\Rightarrow \frac{1}{2} C s V_{dc}^{2} + K_v V_{dc}^{2} = K_v V_{dc}^{*2}$$

$$\Rightarrow \left(\frac{1}{2} C s + K_v\right) V_{dc}^{2} = K_v V_{dc}^{*2}$$

$$\Rightarrow \frac{V_{dc}^{2}}{V_{dc}^{*2}} = \frac{K_v}{K_v + \frac{Cs}{2}} \quad .$$

Assuming the structure of the controller K_v as $K_p + \frac{K_i}{s}$ and by substituting this in to the above transfer function

$$\frac{V_{dc}^{2}}{V_{dc}^{*2}} = \frac{K_p + \frac{K_i}{s}}{K_p + \frac{K_i}{s} + \frac{Cs}{2}}$$

$$= \frac{sK_p + K_i}{Cs^2 + 2sK_p + 2K_i} \quad .$$

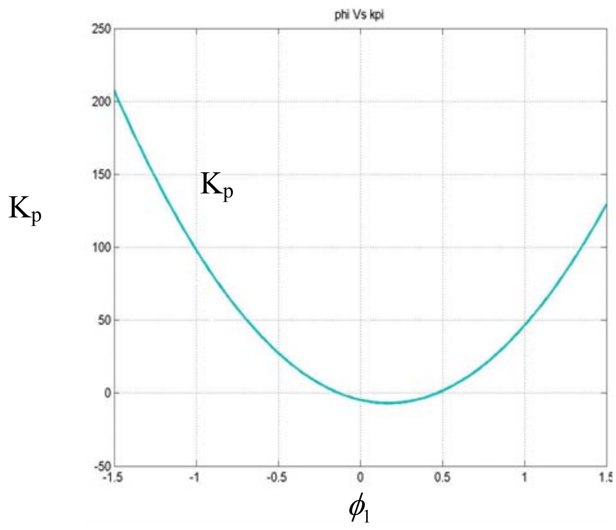

(I)

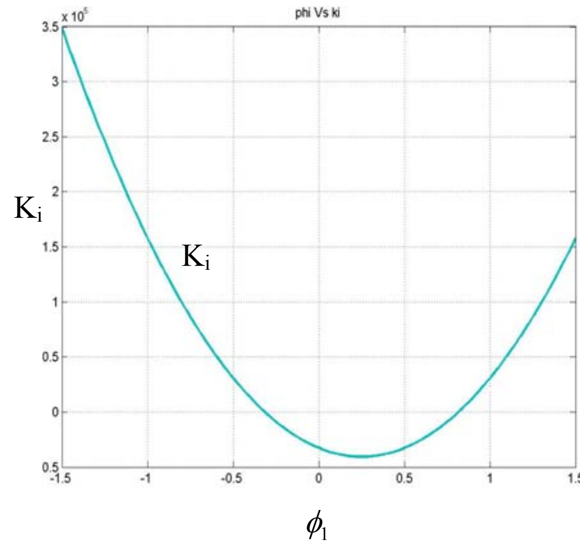

(II)

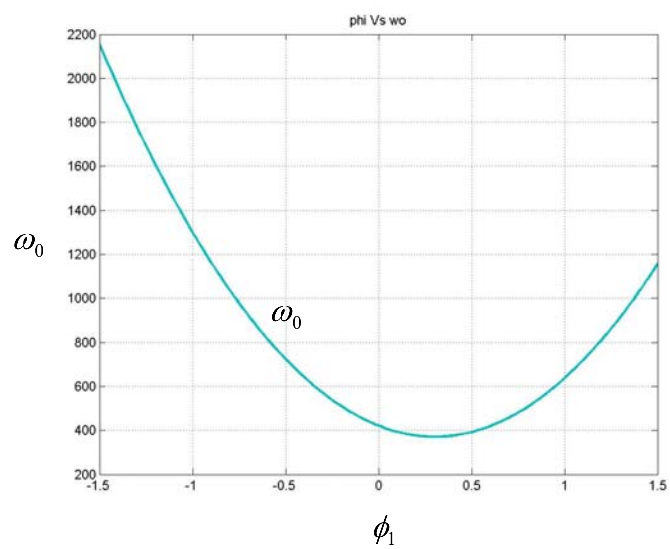

(III)

Figure 5.19: Effect of delay angle ϕ_1 on the control parameters of current controller. (I) K_p (II) K_i (III) ω_o .

Figure 5.19 demonstrates the effect of the delay angle on the control parameters of current controller. The control parameters are determined by varying the delay angle from [- pi / 2 , pi / 2] .

5.11 Circuit Parameters

Unbalanced Source Impedance Operation:

Input line resistance $R_a = 0.2\Omega$; $R_b = 0.4\Omega$; $R_c = 0.1\Omega$

Input line inductance $L_a = 10mH$; $L_b = 20mH$; $L_c = 5mH$

Input Supply Voltage $v_a = 80\cos(\omega t)$

$$v_b = 80\cos(\omega t - 120^0)$$

$$v_c = 80\cos(\omega t + 120^0)$$

Output dc-capacitance $C = 2200\mu F$

Load resistance $R_L = 75\Omega$

Unbalanced Source Voltage and Source Impedance Operation:

Input line resistance $R_a = 0.2\Omega$; $R_b = 0.4\Omega$; $R_c = 0.1\Omega$

Input line inductance $L_a = 10mH$; $L_b = 20mH$; $L_c = 5mH$

Input Supply Voltage $v_a = 80\cos(\omega t)$

$$v_b = 60\cos(\omega t - 120^0)$$

$$v_c = 70\cos(\omega t + 120^0)$$

Output dc-capacitance $C = 2200\mu F$

Load resistance $R_L = 75\Omega$

5.12 Simulation Results

The proposed control scheme is simulated to validate the control methodology. In this, two cases are simulated for unbalanced source impedance with balanced source voltages and the other with unbalanced voltages and unbalanced impedance. Figures 5.20 – 5.21 shows the simulation results of the control scheme of the two-level rectifier with unbalanced source impedance. In the control scheme the reference dc bus voltage is taken as 200 V. Figure 5.20 (I) shows the three-phase modulation signals, which when modulated using the carrier-based PWM generates the switching for the power devices. Figure 5.20 (II) shows the dc bus regulation and it is clear that the controller regulates the dc bus voltage effectively. Figure 5.21 (I) (a) (b) (c) illustrates tracking of the reference currents and demonstrates the effectiveness of the current controller even under unbalanced conditions. The other objective of the control scheme is the constant power transfer and it can be observed in Figure 5.21 (II). Figures 5.22 – 5.23 show the simulation results of control scheme for the unbalanced source impedance and source voltages. The simulation results illustrate the effectiveness of the control scheme both in the balanced and unbalanced operation of two-level rectifier.

Unbalanced Source Impedance Operation:

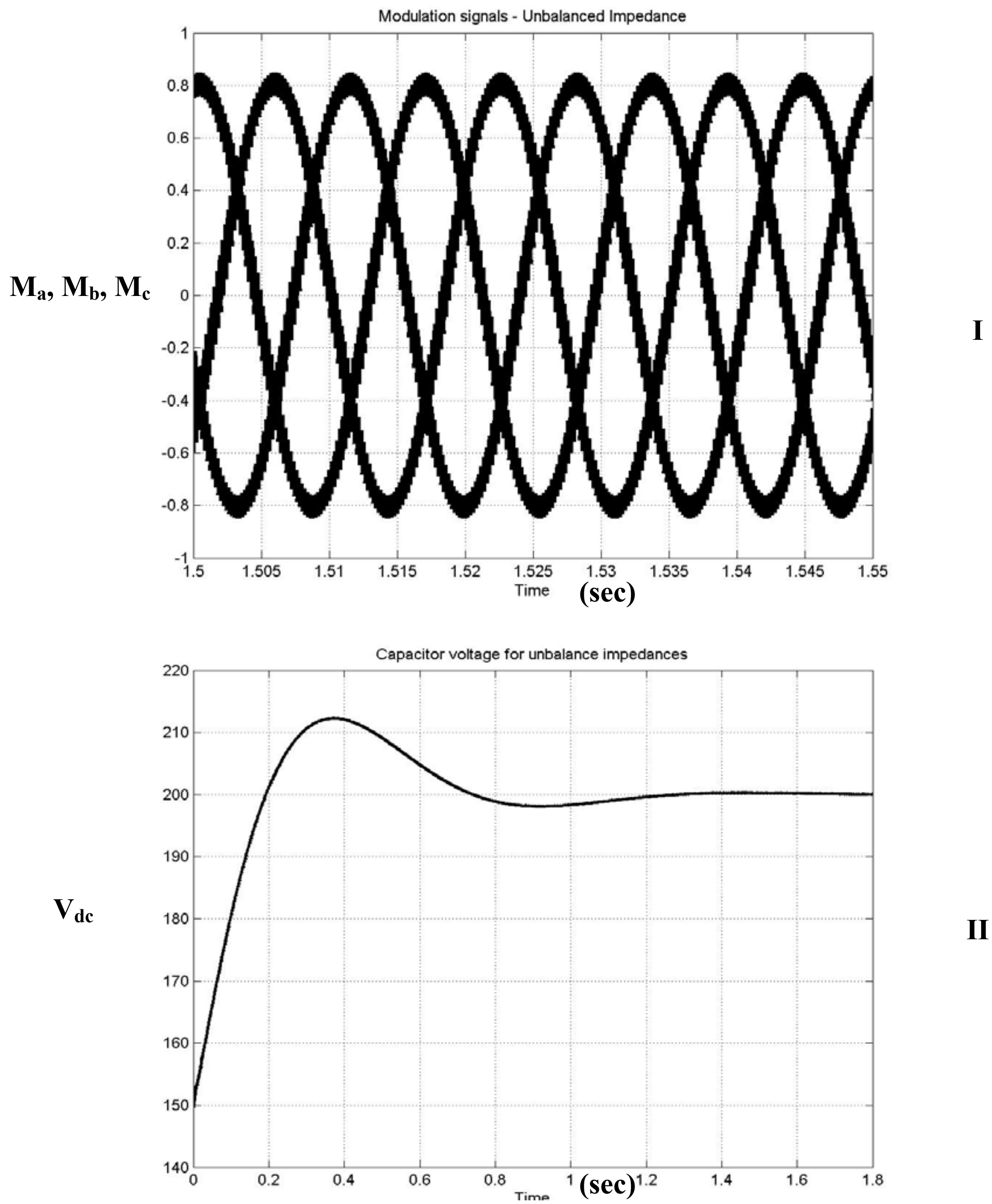

Figure 5.20: Simulation of the control scheme of two level rectifier with unbalance source impedance (I) Three-phase modulation signals (II) Capacitor voltage V_{dc}.

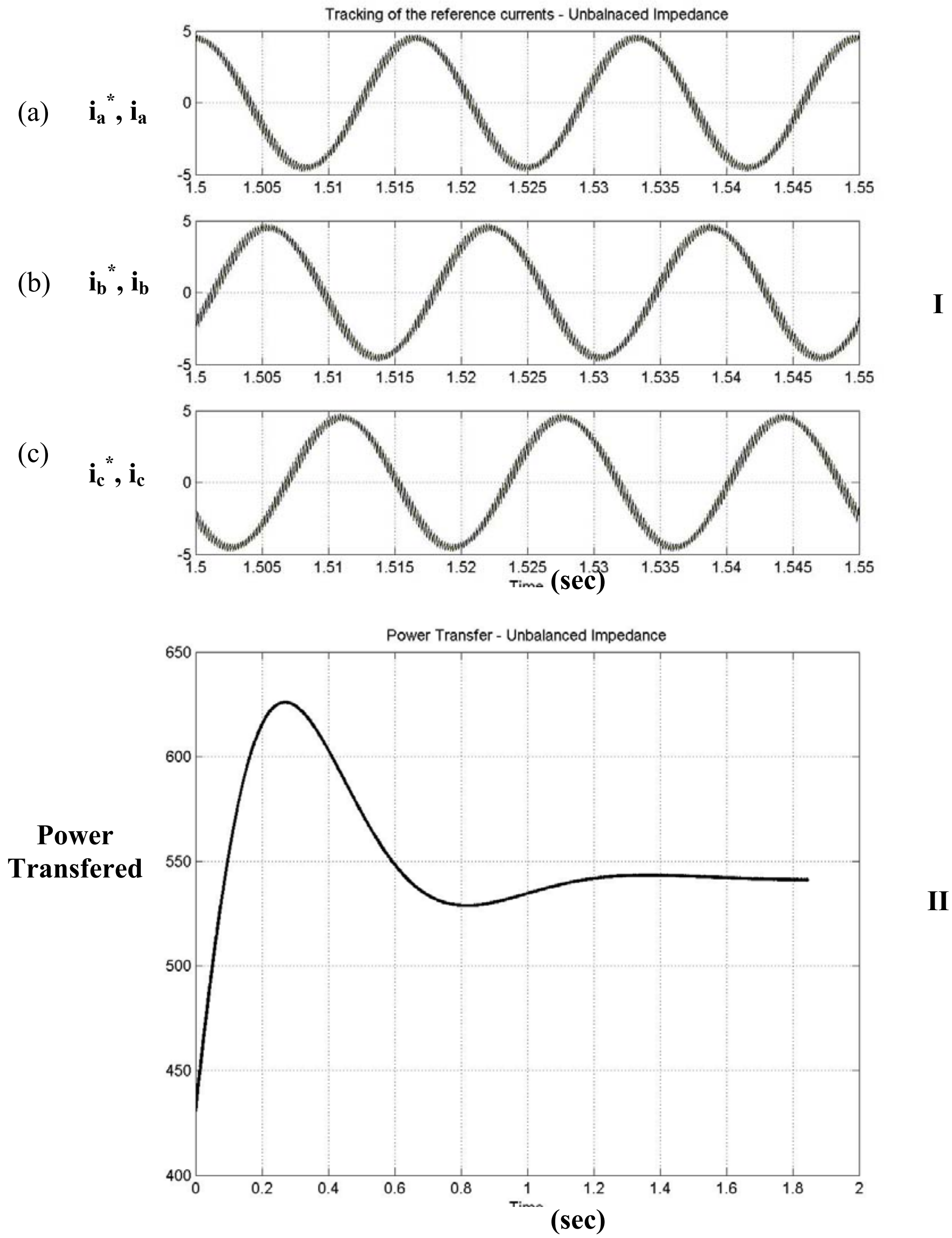

Figure 5.21: Simulation of the control scheme of two level rectifier with unbalance source impedance (I) Tracking of the three phase reference currents (II) Power transferred (P).

Unbalanced Source Voltage and Unbalanced Impedance Operation:

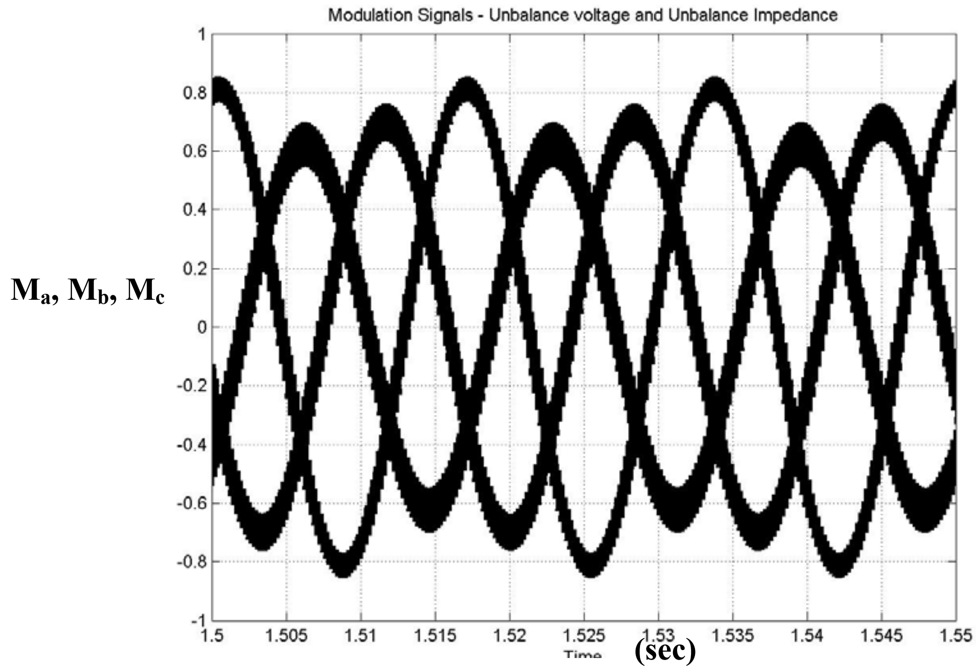

I

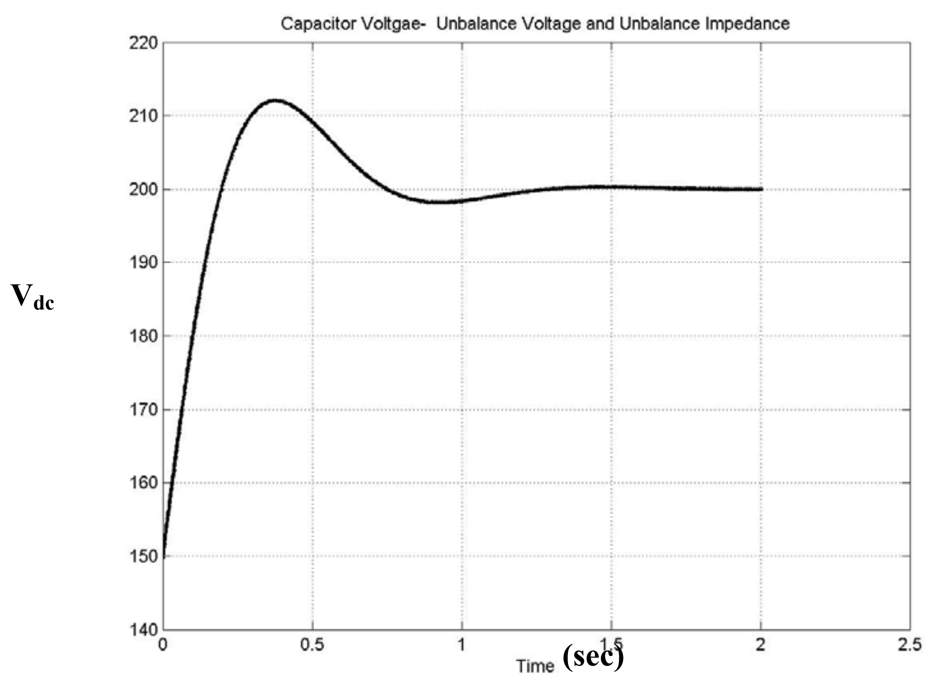

II

Figure 5.22: Simulation of the control scheme of two level rectifier with unbalance source voltage and source impedance (I) Three-phase modulation signals (II) Capacitor voltage V_{dc}.

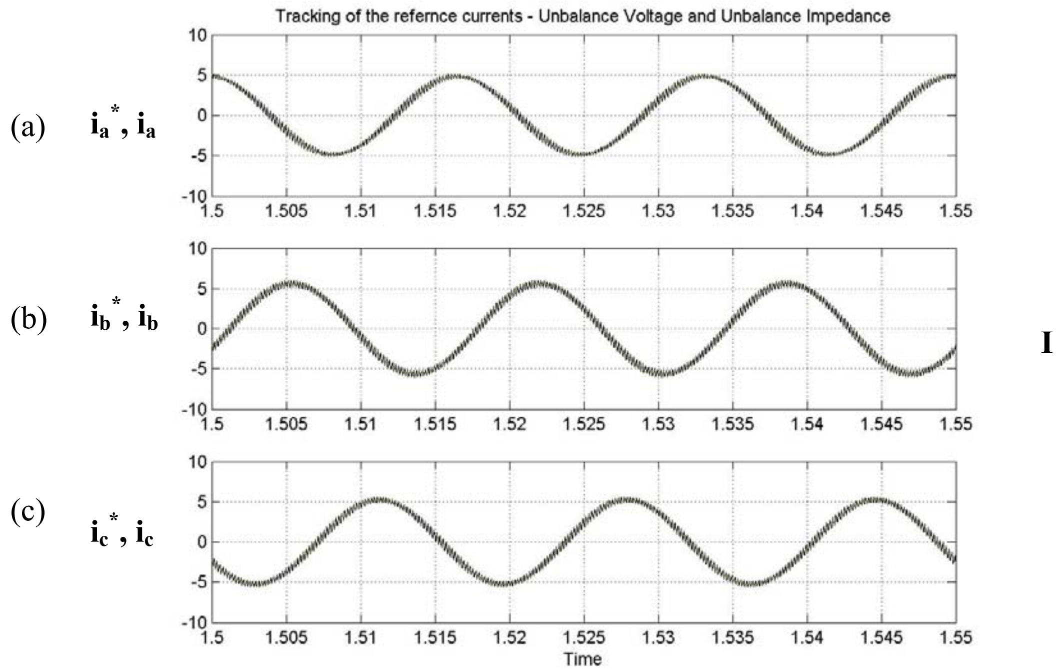

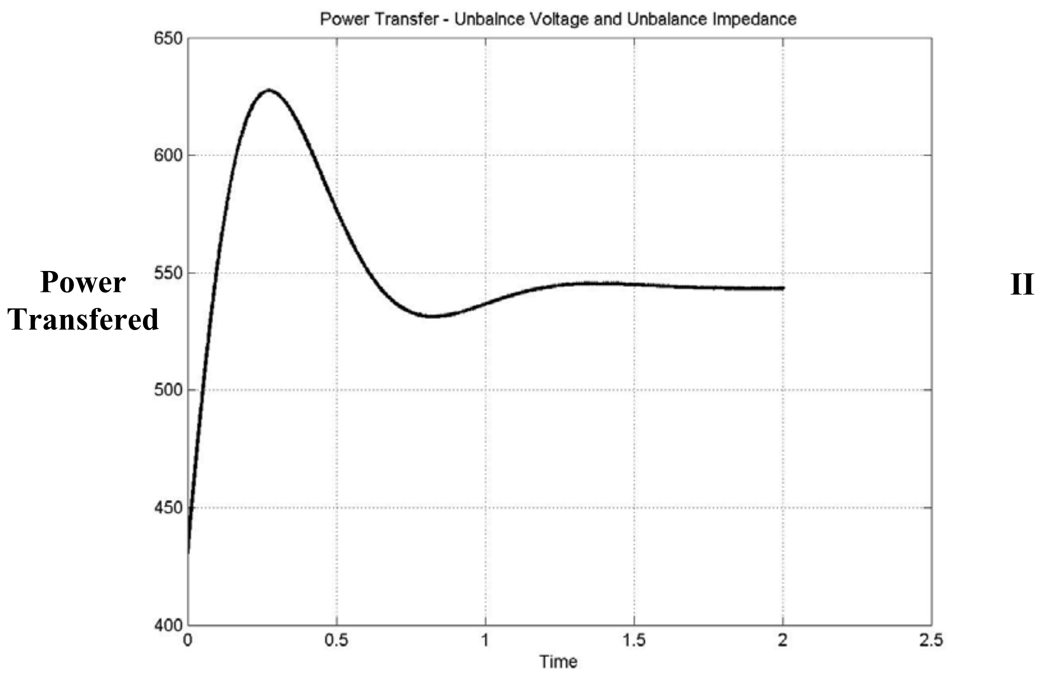

Figure 5.23: Simulation of the control scheme of two level rectifier with unbalance source impedance (I) Tracking of the three phase reference currents (II) Power transferred (P).